

# We are IntechOpen, the world's leading publisher of Open Access books Built by scientists, for scientists

4,800

Open access books available

122,000

International authors and editors

135M

Downloads

Our authors are among the

154

Countries delivered to

TOP 1%

most cited scientists

12.2%

Contributors from top 500 universities



WEB OF SCIENCE™

Selection of our books indexed in the Book Citation Index  
in Web of Science™ Core Collection (BKCI)

Interested in publishing with us?  
Contact [book.department@intechopen.com](mailto:book.department@intechopen.com)

Numbers displayed above are based on latest data collected.  
For more information visit [www.intechopen.com](http://www.intechopen.com)



---

# Ion Synthesis of SiC and Its Instability at High Temperatures

---

Kair Kh. Nussupov and Nurzhan B. Beisenkhanov

Additional information is available at the end of the chapter

<http://dx.doi.org/10.5772/51389>

---

## 1. Introduction

As is known, such advantages of silicon carbide as a high hardness (4th place after diamond) [36, 37], high chemical and radiation resistance, high melting point, etc. became the basis of its wide application not only in microelectronics [1], but also as refractory and abrasive materials. Silicon carbide is included in the oxidation resistant composite materials [42] used in coating system for "Space Shuttle", capable of withstanding temperatures up to 1500°C at the entrance of the ship into the atmosphere. In many attempts to develop an effective oxidation-protection coating for carbon-carbon composites with excellent mechanical properties at elevated temperature, silicon carbide coating has shown the best performance for short periods of up to 1900K [39]. For longer periods and higher temperature applications, a challenging coating system should be developed.

Silicon carbide is regarded by researchers as a suitable material for the front wall structures of fusion reactors. The boers, cutting disks, grinding paper of SiC can be used for boring, drilling, surface grinding and cutting of steel, nonferrous metals, natural stone, concrete, wood and plastic.

The stability of silicon carbide to high temperature treatment is of special interest. As a special application, silicon carbide can be thermally oxidized in the form of SiO<sub>2</sub>, and the devices which can be easily fabricated on Si substrate (Power MOSFET, IGBT, MOS controlled thyristor, etc.) can also be fabricated on SiC substrate [23]. In paper [23] the parabolic growth of thickness of thermal oxide versus oxidation time was observed, and the slope of the plots increases with increasing temperature. The thickness values of oxide films were about 23-77 nm (Si-face, wet oxidation), 18-63 nm (Si-face, dry oxidation), 210-810 nm (C-face, wet oxidation) and 125-260 nm (C-face, dry oxidation) for oxidation time 6 h and depend on temperature value (1000, 1050, 1110 or 1150°C).

Doped with different impurities, silicon carbide is used in semiconductor technology [63, 12].

Field-effect transistors, diodes and other electronic devices based on SiC have several advantages compared to similar silicon devices, for example, the opportunity to work at temperatures up to 600°C, high speed and high radiation resistance. A large number of polytypes of SiC makes it possible to create heteropolytype structures [31, 32, 33]. Currently, using the methods of vacuum sublimation [48], molecular beam epitaxy [15], the epitaxial and heteropolytype layers based on the cubic 3C-SiC and two hexagonal 6H-SiC, 4H-SiC on substrates of SiC, are grown. Heteroepitaxial layers of 3C-SiC on substrates of Si by chemical vapor deposition (CVD) [41] are grown. At the temperatures below 1200°C there are conditions for the growth of both poly- and nanocrystalline SiC with different degrees of crystallinity and structure of the cubic polytype 3C-SiC. Such conditions were realized in the magnetron sputtering [25, 56], laser ablation [53] and plasma deposition [36], plasma-enhanced chemical vapor deposition [19, 43], molecular beam epitaxy [16]. At temperatures below 1500°C in the direct deposition of carbon and silicon ions with energy of ~100 eV, the growth of nanocrystalline films with a consistent set of the polytypes 3C, 21R, 27R, 51R, 6H is possible [49, 50, 51].

In recent years there has been an intensification of studies on the synthesis of SiC by high-dose carbon ion implantation into Si [37, 35]. In addition, the synthesis of SiC by high dose implantation of carbon ions into silicon is also of fundamental scientific interest due to the wide practical application [9 - 11, 47], for example, to create a coating and insulating SiC layers in the manufacture of integrated circuits. High quality crystalline  $\beta$ -SiC film on SiO<sub>2</sub> can be obtained by multiple implantations of carbon ions into silicon and subsequent selective oxidation of the top layer of Si [52]. Intensively developing area is the formation by this technique in SiO<sub>2</sub> of nanostructured systems with inclusions of nanocrystals and clusters of Si, SiC and C, providing at the expense of size effects luminescence throughout the visible spectrum [57]. The study of the stability of these films to high temperature treatment is also of special interest.

The ion synthesis of silicon carbide and studies of crystallization process attract attention of researchers [12, 35, 37, 63]. The implantation of single energy carbon ions with a Gaussian distribution on the depth in silicon is of interest due to a presence of wide range of nanolayers with different concentrations of carbon and silicon atoms and, therefore, a presence of different clusters and nanocrystals of silicon, carbon and silicon carbide in the implanted layer after implantation and annealing. The properties of these layers have been investigated in detail. In previous investigations, the carbon ions with energy of 40 keV were used for considered purposes in a number of papers [8, 13, 20], and doses ranged 10<sup>16</sup>-10<sup>18</sup> cm<sup>-2</sup> were used in almost all of investigations, when the ion synthesis of a silicon carbide film was carried out [2]. The IR absorption technique was widely applied for the investigation of these layers [26, 55]. It has been used, mainly, to confirm the formation of silicon carbide in the implanted layer and, to obtain the new information about the layer structure as well. In some papers, the dependence of both shift of the wave length of a minimum of IR transmission peak and the change of its half width versus the annealing temperature are used for interpretation of IR transmission spectra. In our opinion, it is necessary to investigate such

important characteristics as a change of an area under a curve of IR transmission spectrum band and a change of peak amplitude at  $800\text{ cm}^{-1}$  versus the annealing temperature which contains very valuable information about the structure changes in an implanted layer. If the thickness of ion-synthesized film is comparable or smaller than the wavelength of incident electromagnetic radiation, under certain geometric conditions of the experiment, one can observe not only the transverse optical oscillations of atoms (TO-phonons), as well as longitudinal optical lattice oscillations (LO-phonons) [3]. The detection of LO-phonon peak of SiC and its change after film annealing give additional information on the crystallization processes. It is necessary to carry out the circumstantial investigations devoted to an analysis in detail of change in a wider temperature interval of an half width of IR transmission peak which characterizes the degree of structure order of an ion implanted layer.

In the majority of analogous studies, the post-implantation isochronous annealing of samples was carried out at temperatures from 400 up to  $1200^{\circ}\text{C}$  [11, 14, 2, 27]. However, in several studies [28, 47] the temperature range was extended and, the ion implanted layers had been annealed at temperatures 1300 and  $1405^{\circ}\text{C}$ . We believe also, that the temperature interval  $400\text{--}1200^{\circ}\text{C}$  is not sufficient for a annealing of disordered layer and completion of crystallization processes. A more detailed investigation of processes at temperatures ranged from 20 up to  $1405^{\circ}\text{C}$  permits to observe a number interesting effects taking place in an implanted layer.

The authors of papers [11, 2, 5, 55] declare about a significant diffusion of carbon and, contrariwise, that is negated in works [13, 26, 27]. The authors of papers [8, 4, 47, 34] show that a layer has the electron conduction after annealing. The data of [28] give of evidence about the p-type conduction.

In a number of studies [6, 2, 5] a synthesis of SiC on a (100) oriented silicon substrate is considered as preferable, but at the same time in papers [13] the orientation (111) of substrate is declared as a most suitable. [4] investigated the optical and photoelectric properties of the SiC-Si structure, formed by implantation into (100), (110) and (111) oriented n- and p-type silicon of  $^{12}\text{C}$  ions with energies of 40 and 70 keV, and doses of  $4.3 \times 10^{17}$  and  $5 \times 10^{17}\text{ cm}^{-2}$ . Analysis of the IR absorption spectra of silicon layers implanted by carbon ions with energy of 70 keV allowed finding a significant dependence of crystallinity of the SiC layer on the orientation of the substrate after annealing at temperatures of  $700\text{--}900^{\circ}\text{C}$ . Although the tetrahedral Si-C-bonds more intense formed at an orientation of the substrate (100), annealing at  $1100^{\circ}\text{C}$  all evens out differences in the absorption spectra for all three substrate orientations (100), (110) and (111). The photovoltage photoresponse was obtained in all implanted structures. Investigation of current-voltage characteristics showed improvement in the rectification effect of the structure after annealing. The possibility of creating of  $\beta\text{-SiC-Si}$  heterostructures by ion implantation technique (band gap of 2.39 eV and 1.11 eV, respectively) was shown.

Frangis et al. [17, 18] formed  $\beta\text{-SiC}$  in silicon by high-temperature implantation ( $850\text{--}950^{\circ}\text{C}$ ) of carbon ions with energies 200 keV and doses ranged within  $(0.2\text{--}1) \times 10^{18}\text{ cm}^{-2}$ . Implantation was carried out into silicon wafers of orientation (100) and (111). In both cases,  $\beta\text{-SiC}$  was formed with the same orientation as the matrix. It also reported that implantation at a lower temperature ( $500^{\circ}\text{C}$ ), but at higher energy (300 keV) leads to the formation of good quality  $\beta\text{-SiC}$ .



Aleksandrov et al. [6] carried out the synthesis of single-crystal SiC layer with one-step technique of high current ion implantation of carbon atoms into silicon substrates with orientations (001) and (111). Single crystal layer of SiC, which contains a small number of twins, was synthesized by the implantation of carbon ions with dose of  $6 \times 10^{17} \text{ cm}^{-2}$  into (001) oriented silicon wafer using a focused ion beam with current density of  $300 \text{ A/cm}^2$ . When the ion current density was  $150 \text{ A/cm}^2$ , a single crystal SiC layer with a high concentration of twins was formed at the interface with the substrate Si. On top of this layer is formed a layer of polycrystalline SiC. When the implantation of carbon ions was carried out into (111) oriented silicon, single crystal  $\beta$ -SiC layer is not formed even when implanted into substrate heated up to a temperature of  $850^\circ\text{C}$ . Polycrystalline SiC layer at the surface and single-crystal SiC layer with a high density of twins near the interface with the crystal Si matrix, are formed.

This chapter presents the study of silicon carbide and carbon layers on silicon synthesized by ion beam techniques. The investigations of silicon layers implanted by carbon ions with energy  $40 \text{ keV}$  and dose  $3.56 \times 10^{17} \text{ cm}^{-2}$  after annealing over a wide temperature range from  $20$  up to  $1400^\circ\text{C}$  using the special IR analysis are described. The features of change of the SiC-peaks in the spectra of the infrared transmission due to the influence of the Gaussian profile of the distribution of carbon in silicon are shown. Experiments to observe the longitudinal optical oscillations (LO-phonons) associated with the silicon carbide were carried out. A type of a conduction of synthesized silicon carbide was studied. Definite information from a shape analysis of the IR transmission curve was obtained. A particular attention was attracted on some problems which were disputable in previous investigations. IR studies of high-temperature instability of homogeneous layers of silicon carbide on (100) and (111) oriented silicon substrates synthesized by multiple implantation of carbon ions with energies  $E = 40, 20, 10, 5$  and  $3 \text{ keV}$ , are described. By IR spectroscopy, Auger electron spectroscopy and X-ray reflectometry the composition and the processes of structural adjustment of the layer during annealing are analyzed. By ion-beam sputtering and magnetron sputtering techniques the  $\text{SiC}_{0.8}$  and C films on the silicon wafers were deposited. Characteristics of the films by X-ray reflectometry are analyzed.

## 2. Experimental

Carbon implantation was carried out under completely oil-free conditions using elaborated accelerator. A vacuum in the implantation chamber is created by help of the ceolite vacuum pumps ( $6.5 \times 10^{-2} \text{ Pa}$ ) and titan magnet discharge pumps ( $1.3 \times 10^{-4} \text{ Pa}$ ). These pumps permit to except completely the organic compounds in volume which could be to contaminate the surface of the implanting samples. Gas (dioxide of carbon) has been used to obtain the single-charged ions of  $^{12}\text{C}^+$ . The implantation dose was determined by integrating of the beam current registered on the target with suppression of a secondary emission. In order to prevent a sample heating during implantation, the ion current density was kept at a level less than  $3 \text{ mA/cm}^2$ . The temperature of the target during the implantation is controlled by a thermocouple and, it not exceeds  $20\text{--}25^\circ\text{C}$ . The implantation of carbon ions was carried out into single-crystal (100) and (111) oriented silicon wafers of sizes  $7 \times 12 \times 0.4 \text{ mm}^3$  with an electrical resistivity  $4\text{--}5$  and

10 Ohm cm, respectively. After cleaning and removing the native surface oxide in a chemical etch, the samples were mounted in the target chamber of the implanter.

A set of these silicon wafers were implanted by  $^{12}\text{C}^+$  ions with energy 40 keV and dose  $3.56 \times 10^{17} \text{ cm}^{-2}$  at room temperature. To observe the longitudinal optical oscillations (LO-phonons) of atoms in synthesized film, a rotating shaft was incorporated into work chamber of infrared spectrometer. A sample holder is attached on this shaft. This system permits to make the IR transmission measurements of an ion implanted layer versus an angle of incidence of electromagnetic radiation on sample surface over the range  $0\text{-}360^\circ$  with step of  $5^\circ$ . However, in practice, at measuring of spectra we change the angle of incidence from 0 up to  $\pm 75^\circ$ . It was observed no differences in transmission spectra measured from samples sloped to the radiation at a rotation of shaft both clockwise and anti-clockwise from the normal. Isochronous annealing of ion implanted samples was carried out in vacuum over the temperature range  $200\text{-}1400^\circ\text{C}$  with steps of  $50\text{-}200^\circ\text{C}$ . The annealing was carried out in a low-inertia economical vacuum furnace especially elaborated and created for these purposes. It was carried out in conditions of completely oil-free pumping-out at a residual pressure  $\sim 1.3 \times 10^{-4} \text{ Pa}$ . The temperature was controlled by a help of tungsten-rhenium thermocouple.

To obtain a rectangular profile of the distribution of carbon atoms in the silicon, implantation of carbon ions of different energies and doses into second set of single-crystal silicon wafers of n- and p-type of conductivity was carried out sequentially in the following order: 1)  $E = 40 \text{ keV}$ ,  $D = 2.80 \times 10^{17} \text{ cm}^{-2}$ , 2)  $20 \text{ keV}$  and  $0.96 \times 10^{17} \text{ cm}^{-2}$ , 3)  $10 \text{ keV}$  and  $0.495 \times 10^{17} \text{ cm}^{-2}$ , 4)  $5 \text{ keV}$  and  $0.165 \times 10^{17} \text{ cm}^{-2}$ , 5)  $3 \text{ keV}$  and  $0.115 \times 10^{17} \text{ cm}^{-2}$ . The ratio of the concentrations of carbon and silicon atoms in the depth was about  $N_{\text{C}}/N_{\text{Si}} = 0.7$ . Post implantation annealing of the samples was performed in a vacuum in the temperature range  $200\text{-}1200^\circ\text{C}$  for 30 min with a step of  $200^\circ\text{C}$ . Then, the SiC films were subjected to prolonged isothermal annealing at the temperature of  $1200^\circ\text{C}$  for several hours in an atmosphere of inert gas (Ar) and, after specific time intervals infrared transmission spectra were recorded. The IR transmission spectra were recorded in differential regime on double-beam infrared spectrometer ( $400\text{-}5000 \text{ cm}^{-1}$ ). The spectra both at perpendicular incidence of infrared rays on the sample surface and at an angle of  $73^\circ$  with respect to the normal to the sample surface were measured. The composition of the layers was examined by Auger electron spectroscopy. The parameters were as follows: incident electron beam of diameter  $1 \mu\text{m}$ , energy  $10 \text{ keV}$ , angle of incidence  $45^\circ$ , diameter of scanning region  $300 \mu\text{m}$ , vacuum  $1.33 \times 10^{-8} \text{ Pa}$ , angle of  $\text{Ar}^+$  beam incidence  $45^\circ$ . Parameters of films were investigated using the X-ray reflectometry at small glancing angles by recording the angular dependence of the reflection coefficient for two spectral X-ray lines  $\text{CuK}_\alpha$  ( $0.154 \text{ nm}$ ) and  $\text{CuK}_\beta$  ( $0.139 \text{ nm}$ ) at the facility "ComplexXRay C6". Selection of spectral lines  $\text{CuK}_\alpha$  and  $\text{CuK}_\beta$  from polychromatic spectrum was carried out using thin semi-transparent and thick untransparent monochromators, respectively, made from the pyrolytic graphite with a mosaic angle of  $0.5^\circ$ .

SiC films on the silicon substrates ( $25^\circ\text{C}$ ) were also synthesized by ion-beam sputtering of a two-component target of graphite and silicon. The C films on the silicon substrate ( $75^\circ\text{C}$ ) by magnetron sputtering were synthesized. Parameters of SiC and C films on Si substrates were determined using the X-ray reflectometry.

### 3. Results and discussion

#### 3.1. A model of an carbon implanted silicon layer and the mechanism of the low temperature formation of Si- and SiC crystallites

In Fig.1 the calculated profile of carbon atom distribution in Si constructed basing on data  $R_p$  and  $\Delta R_p$  from [21] are presented. The Gaussian profile (Fig.1, curve 1) was calculated for the implantation of carbon ions with energy 40 keV and dose  $3.534 \times 10^{17} \text{ cm}^{-2}$ , when the carbon concentration in the distribution peak is equal to stoichiometric composition of SiC, i.e.  $N_C/N_{Si} = 1$ , where  $N_C/N_{Si}$  is the ratio of the concentrations of C and Si atoms. The curve 2 in Fig.1 shows the calculated profile, corresponding to dose  $D = 3.56 \times 10^{17} \text{ cm}^{-2}$  of carbon ions used in this investigation.

##### 3.1.1. LO-phonons and their applications to analysis of an implanted layer

As it is well known [45, 66], during interaction of electromagnetic waves with an infinite crystal lattice, the transversal optical oscillations (TO-phonons) of atoms are excited. In overwhelming majority of previous investigations, the synthesis of silicon carbide was identified by help of spectra of transversal optical phonons. No attempts was made to detect the longitudinal optical oscillations (LO-phonons) of atoms of lattice for a Gaussian concentration profiles of carbon in spite of that majority of studies in the field of ion synthesis of silicon carbide was carried out using these profiles. [3] found that an absorption at wave number  $980 \text{ cm}^{-1}$  is observed, if the angle of incidence of irradiation on the sample surface deviate from perpendicularity. Implantation of carbon ions with energies of 24 and 40 keV and a dose of  $4.3 \times 10^{17} \text{ cm}^{-2}$  carried out at room temperature into a (111) oriented Si plate of p-type conductivity. Annealing was performed in a vacuum at temperatures of 900 and 1100°C for 30 minutes. The presence in the transmission spectrum of bands associated with the LO-and TO-phonons made possible to calculate such parameters of SiC, as high frequency,  $\epsilon_{\infty}$ , and the low-frequency dielectric constant,  $\epsilon_0$ , attenuation coefficient of the phonons, the effective charge  $e^*/e$  and the force constant  $\rho$ . So, the detection of LO-phonons may be used to obtain additional information about a structure of ion implanted layer. Moreover, the frequency values of both the transversal- and longitudinal oscillations permit to determine the parameters of efficient charge which is a quantitative criterion of a compound polarity. The efficient charge value permits to calculate a mobility of free charge carriers.

If a thickness of ion synthesized film is less or comparable with a wave length of the electromagnetic radiation incident on film's surface, the limitations related with the condition of infinity of crystal lattice are lifted. As a result, one can to observe the longitudinal optical oscillations of lattice atoms at definite geometrical conditions of experiments [66]. In this relation, the special experiments to observe these phonons were carried out. For this purpose, the IR transmission spectra versus an angle of incidence of electromagnetic radiation on sample surface with step of  $5^\circ$  were measured.

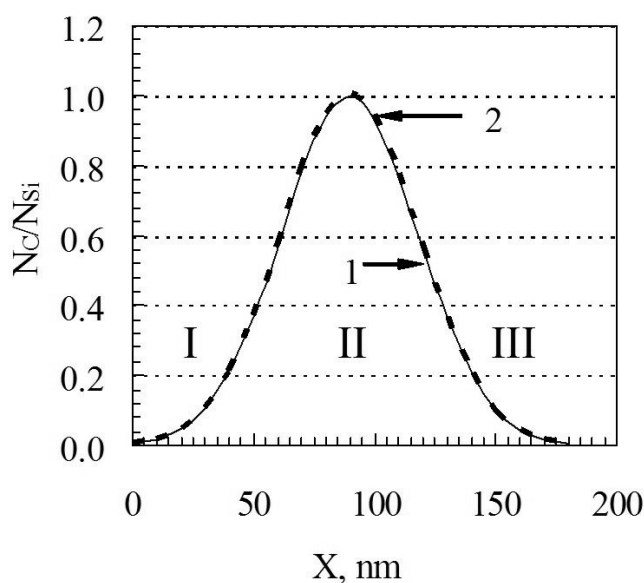


**Figure 1.** The calculated profiles of distribution of carbon atoms in Si constructed basing on data of  $R_p$  and  $\Delta R_p$  from [21]. The energy of carbon ions is 40 keV, dose  $3.534 \times 10^{17} \text{ cm}^{-2}$  (curve 1) and  $3.56 \times 10^{17} \text{ cm}^{-2}$  (curve 2).

In Figs.2 and 3 the IR transmission spectra of both (100)- and (111) oriented silicon samples implanted by carbon ions with energy 40 keV and dose  $3.56 \times 10^{17} \text{ cm}^{-2}$ , after isochronous annealing over the temperature range 200-1400°C, are presented. The spectra at both perpendicular incidence of infrared rays on the sample surface and at an angle of 73° with respect to the normal to the surface were measured. In Fig.4 the wave number values in maximum of IR transmission versus the annealing temperature are presented. The curves on this figure were constructed using the experimental data presented on Figs.2 and 3. The curves for TO-phonons were constructed basing on the infrared transmission spectra measured by using of perpendicular incidence of the infrared rays on the sample surface.

Figs. 2 and 3 show the appearance of an IR absorption peak at 965-970  $\text{cm}^{-1}$  in the spectra from samples inclined to IR irradiation at an angle of 73° with respect to the normal to the sample surface. This absorption peak begins to be appeared after annealing at 1000°C for both types of substrate orientation together with the main peak at 797-800  $\text{cm}^{-1}$  which corresponds to the transversal optical atomic oscillation of SiC. Basing on the values of wavelength of this peak, its amplitude and synchronous modification together with the peak for transversal optical oscillation of SiC during annealing as well, the peak at 965-970  $\text{cm}^{-1}$  was associated with longitudinal optical phonons of silicon carbide. The temperature of LO-phonon appearance is about 300°C higher, than that for TO-phonons of SiC (700°C). It may be caused by smallness of the LO-phonon peak amplitude and, in consequence of this, by difficulties of their registration.

For (100) oriented substrates, the increase of the annealing temperature over the range 1000–1350°C leads a linearly increase of LO-phonon wavelength at minimum of amplitude from 930 to 965  $\text{cm}^{-1}$  and, then wavelength increasing is saturated. As for (111) oriented sub-

strates, unlinearly increase of LO-phonon wavelength in the range 955–970  $\text{cm}^{-1}$  up to 1400°C is observed. Thus, the formation of SiC crystallites, i.e. the intensive formation of Si-C tetrahedral bonds of necessary length and bond angles, in the case of (111) oriented substrate is not completed up to the silicon melting point, as for (100) oriented substrate that is completed at 1350°C. The difference between the LO-phonon curves behaviour for (100) and (111) oriented substrates indicates on the differences in the crystallization mechanism. One can see an influence of silicon substrate orientation on SiC crystallization in the implanted layer from the TO-phonon curve also (Fig.4).

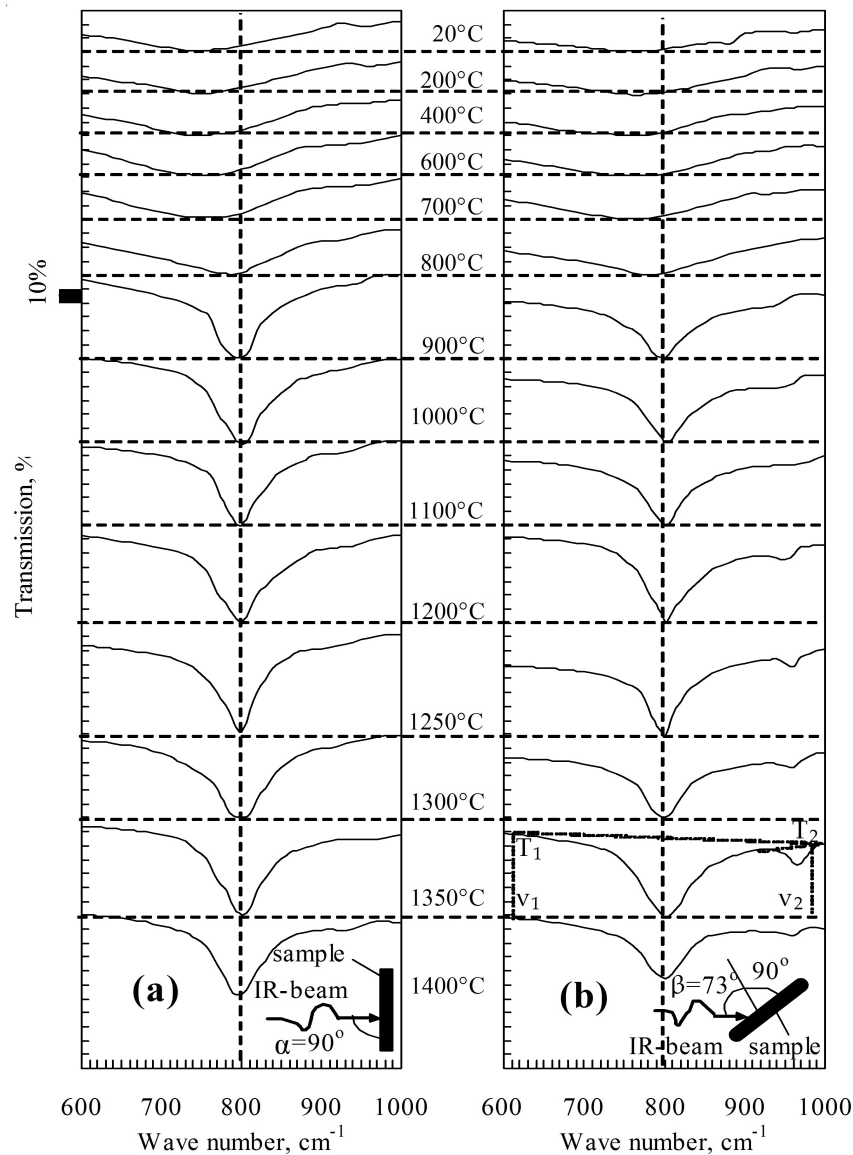


**Figure 2.** The IR transmission spectra of (100) oriented Si samples implanted by  $^{12}\text{C}^+$  ions ( $E = 40 \text{ keV}$ ,  $D = 3.56 \times 10^{17} \text{ cm}^{-2}$ ), after isochronous annealing over the temperature range 200–1400°C: a)  $\alpha = 90^\circ$ ; b)  $\beta = 73^\circ$ .



In some investigations no changes in the IR transmission spectra after annealing at 700°C [8], 850°C [14], 875°C [11], 900°C [26], 1100°C [2] were observed. That was explained by finishing of the  $\beta$ -SiC formation process. Really, that may be correct, if we are based on the analysis of TO-phonon curve only. However, as is seen from Fig.4, the TO-phonon curves show the saturated absorption and give no additional information over the temperature range of 900–1400°C, as the LO-phonon curves undergo the substantial changes at these temperatures indicating on the structural changes in the ion implanted layer. Thus, one can conclude that the observation and measurement of LO-phonon peak are important for an analysis of crystallization process.

As it is known [38], the TO- and LO-phonons frequencies are bounded with the equation:

$$\frac{\nu_{LO}}{\nu_{TO}} = \left( \frac{\epsilon_0}{\epsilon_\infty} \right)^{1/2} \quad (1)$$

Where  $\epsilon_0$  and  $\epsilon_\infty$  are the low-frequency and the high-frequency dielectric constants, respectively. The effective charge  $e^*/e$  is determined from the equation [54]:

$$\frac{e^*}{e} = \left( \frac{\epsilon_0 - \epsilon_\infty}{4\pi} \right)^{1/2} \left( \frac{M_n}{N} \right)^{1/2} \left( \frac{3\omega_0}{\epsilon_\infty + 2} \right) \quad (2)$$

$$\left( \frac{\pi(\epsilon_0 - \epsilon_\infty)M_n\nu_{TO}^2}{N e^2} \right)^{1/2} \left( \frac{3}{\epsilon_\infty + 2} \right)$$

where  $\omega_0$  is the resonance frequency,  $N = 4.84 \times 10^{22} \text{ cm}^{-3}$  is the concentration of ion pairs,  $M_n = (M_+M_-)/(M_+ + M_-) = 1.396 \times 10^{-23} \text{ g}$  is the reduced mass of ion pair,  $\nu_{TO} = 2.395 \times 10^{13} \text{ cm}^{-1}$  is the frequency of TO-phonon irradiation.

The dimensionless parameter,  $\rho$ , which is proportional to the absorption quantity, is determined from the equation:

$$\rho = \frac{\epsilon_0 - \epsilon_\infty}{4\pi} \quad (3)$$

The values of  $\epsilon_0$ ,  $e^*/e$  and  $\rho$  determined from the equations (1)–(3) are equal to 9.82, 0.89, and 0.25, respectively. The value of  $\epsilon_\infty$  has been chosen to be equal to 6.7, because according to [45] the sufficiently great dispersion of this value leads an insignificant changes. So, both the detection and the measuring of LO-phonons have been permitted to determine some characteristics of synthesized film.

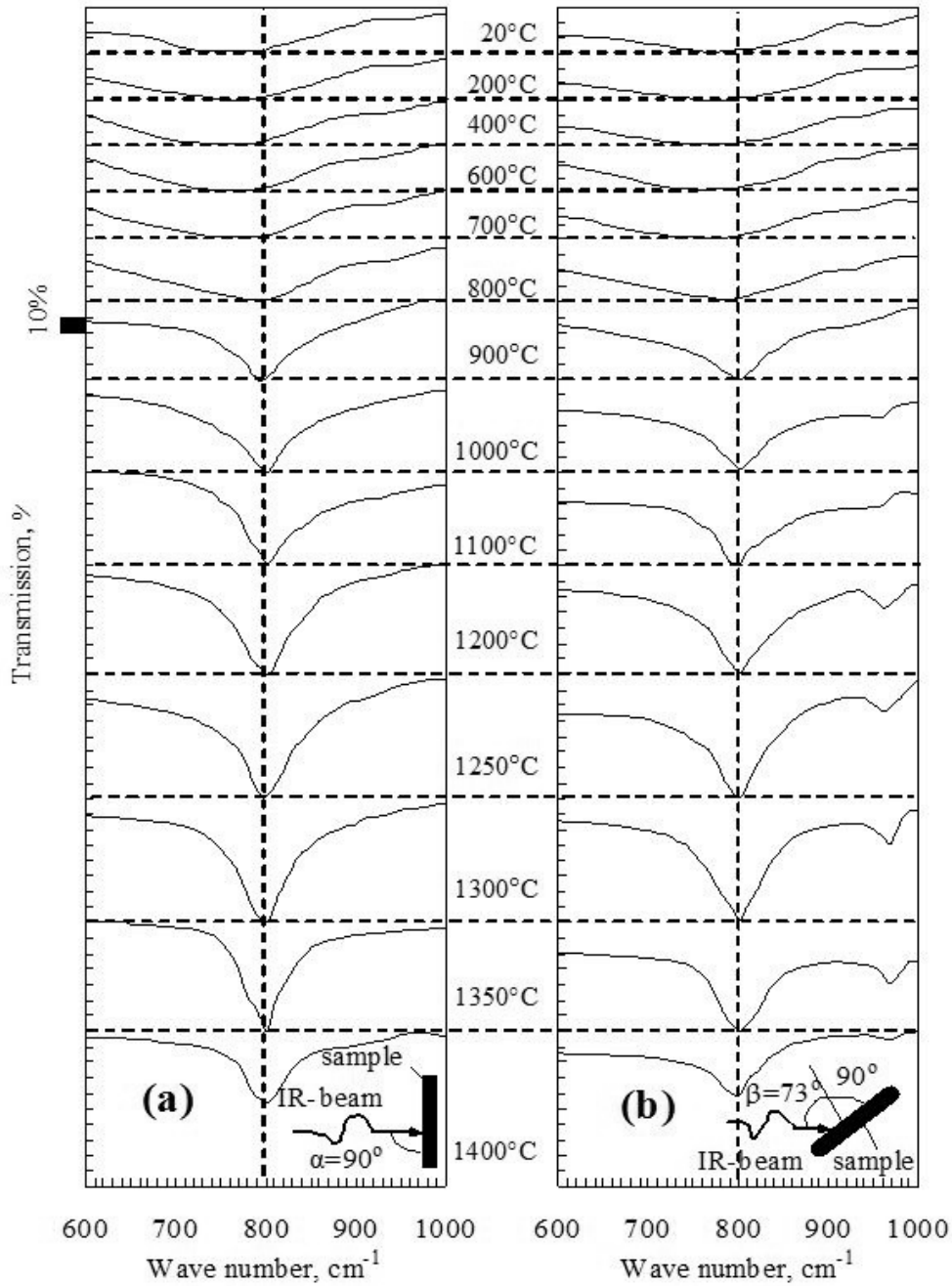


**Figure 3.** The IR transmission spectra of (111) oriented Si samples implanted by  $^{12}\text{C}^+$  ions ( $E = 40 \text{ keV}$ ,  $D = 3.56 \times 10^{17} \text{ cm}^{-2}$ ), after isochronous annealing over the temperature range 200–1400°C: a)  $\alpha = 90^\circ$ ; b)  $\beta = 73^\circ$ .

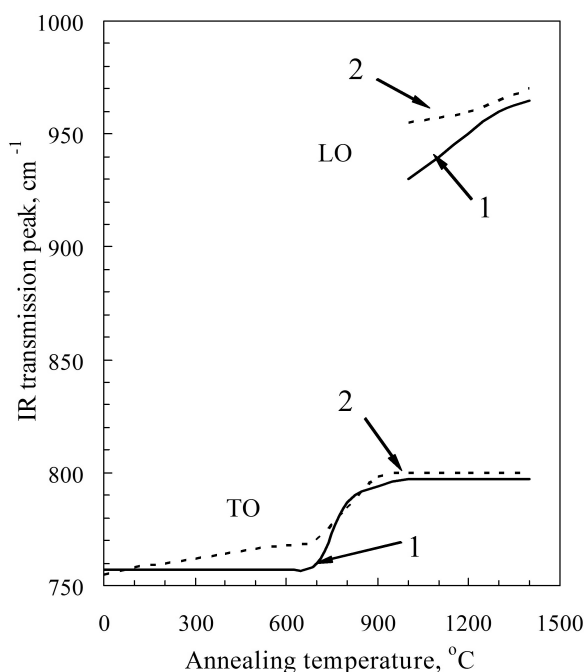


**Figure 4.** Wave numbers of IR transmission minimum for TO- and LO-phonon peaks of SiC versus an annealing temperature for carbon implanted silicon layers on Si substrates ( $E = 40$  keV,  $D = 3.56 \times 10^{17} \text{ cm}^{-2}$ ): 1 - Si(000); 2 - Si(111).

### 3.1.2. The IR transmission analysis of ion-implanted layer on (100) and (111) oriented silicon

In Figs.5a and b, the values of amplitude and halfwidth (FWHM) of the IR transmission peak, respectively, versus an incidence angle of the infrared radiation on the carbon implanted (100) oriented silicon samples, are presented. These data were obtained after isochronous annealing of samples over the range 200-1200°C for 30 min with the step of 200°C. Beginning from an angle  $\alpha = 50^\circ$  (Fig.5a), almost linear decreasing of TO-phonon peak amplitude and simultaneous increasing of LO-phonon peak amplitude are observed. The changes of LO- and TO-phonons peak amplitudes are correlated with one another.

The halfwidth (FWHM) changes of the peak have a more complicated dependence from the incidence angle of the infrared radiation on the sample surface (Fig.5b). This dependence has no correlation with the data in Fig.5a. The half-width of the peak is usually dependent on the quality of the crystal structure of the film and should not depend on the angle of incidence of IR radiation. Apparently, the decreasing of halfwidth of the TO-phonon peak can be explained by the presence of non-tetrahedral Si-C-bonds of a certain type, which are oriented in the space of the film in such a way that with increasing angle  $\alpha$  above  $35^\circ$  they cease to absorb infrared radiation at frequencies near  $800 \text{ cm}^{-1}$ . This is equivalent to the effect of decay of these bonds, since it leads to a decrease in the amplitude and the narrowing of the TO-phonon peak, but can not testify about improving the structure of the layer. This is also accompanied by the appearance of deformed LO-phonon peak in the frequency range near  $950 \text{ cm}^{-1}$ . With the increase of the angle  $\alpha$  up to  $73^\circ$ , the narrowing of LO-phonon peak

and an increase in its amplitude are taken place. The interpretation of these results requires further investigation.

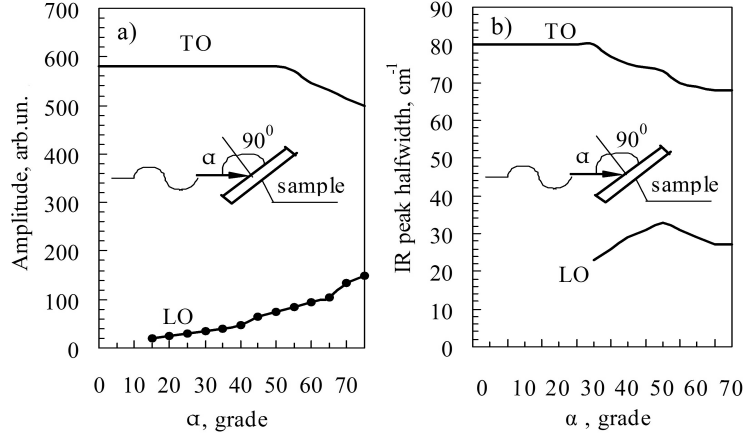


**Figure 5.** Amplitude (a) and halfwidth (FWHM) (b) of TO- and LO-phonons peaks of SiC of the IR transmission versus the incidence angle of IR radiation on the surface of the carbon implanted Si.

In previous IR investigations of implanted by  $^{12}\text{C}^+$  ions silicon layers, a shift in frequency of an absorption maximum versus the annealing temperature, and also the changes of half-width and amplitude of peak were observed. Analyzing the IR transmission spectra presented in Figs.2 and 3, one can see not only the changes of these parameters. A base-line to each spectrum (Fig.2, 1350°C) was drawn. As is seen, the areas of obtained figures are changed, too (Fig.6). In our opinion, the area under the IR transmission curve is associated with the number of absorbing objects in the ion-implanted layer and better shows the transformation of these objects during isochronal annealing. As the object may be not only the crystallites of SiC, but also the another types of infrared active compounds of carbon atoms with carbon or silicon atoms, and silicon atoms one with another, which one can unify under one common appellation - clusters.

Basing on the mentioned above, the IR transmission spectra (Figs.2 and 3) were analyzed in detail accordingly to all listed points. In Fig.6 an area of the IR transmission peak (see Fig.2) associated with TO-phonons of SiC obtained both at perpendicular incidence of infrared rays on the sample surface (curve 1) and at an angle of  $73^\circ$  with respect to the normal to the sample surface (curve 2), versus the annealing temperature are presented. Area values can be determined by direct measurement or by using the expression (Fig.2, 1350°C):

$$A = \frac{1}{2}(T_1 + T_2)(\nu_2 - \nu_1) - \int \tau(\nu) d\nu \approx \frac{1}{2}(T_1 + T_2)(\nu_2 - \nu_1) - \sum \tau(\nu) \delta\nu \quad (4)$$

where  $A$  – total absorption (or transmission) in relative units in the wave number range  $\nu_1 < \nu < \nu_2$ ,  $\tau(\nu)$  – transmission at frequency  $\nu$ ,  $T_1$  and  $T_2$  – the values of IR transmission at wave numbers  $\nu_1$  and  $\nu_2$ , respectively,  $\delta\nu$  – step of measurements, equal to 2.5 or 5  $\text{cm}^{-1}$ . The areas

corresponded to LO-phonons have been not measured due to of their infinitesimal. Further the data obtained for a perpendicular incidence of IR-rays on sample surface will be discussed, as an analysis of the curve 2 is difficult due to the absence of the reflection data. As is seen from Fig. 6 (curve 1), the four peaks at 600, 1000, 1200 and 1350°C are evidently observed, which, seemingly, are related with four physical processes occurring in ion implanted layer in four temperature ranges. The same maxima are observed for curve 2 in approximately the same temperature ranges. On this curve a fifth maximum at 200°C is also observed.

It is necessary to note, that in most previous investigations, mainly, the informations corresponding to the peak in range 900-1000°C are obtained using the dependences of halfwidth and a shift in frequency of an absorption maximum from the annealing temperature. The physical processes corresponded to the peaks of both 600 and 1200-1400°C have not been studied in detail, partly, due to the hard access of the temperature range of 1200-1400°C and, partly, due to weak defined processes at 600°C. It follows from the Fig.6 that the change of area of SiC-peak takes place over the whole temperature range from 20°C up to 1400°C.

In Fig.7 the values of IR transmission amplitude for TO-phonons of SiC at wavenumber 800  $\text{cm}^{-1}$  and for LO-phonons of SiC versus an annealing temperature for spectra presented in Figs.2 and 3 (curves 1, 1' – for the perpendicular incidence of IR rays on sample, the curves 2, 2', 3, 3' – for an angle of 73°), are shown. When constructing these dependences we have believed that the IR transmission amplitude at 800  $\text{cm}^{-1}$  is proportional to the concentration of tetrahedral oriented Si-C-bonds of atoms incorporated into crystallites of SiC. All factors which can affect on a broadening of peak corresponding to an infinitely thin ideal film of SiC have been neglected. This approximation is to some extent, may distort the true picture of the physical phenomena occurring in ion-implanted layer. However, this assumption is very important in a qualitative sense, since it allows understanding the general course of the process and separating a region of the IR transmission peak [30] due to the contribution of crystallites of SiC in the area value, from a region due to the optically active clusters. As seen in Fig.7, the overall shape of the curves 1 and 2 for the TO-phonons is about the same and has a number of features, in particular, at 1300°C, which is also found on the curve 3 for the LO-phonons. The changes of amplitude take place over the all temperature range from 20 up to 1400°C. There are differences in the crystallization processes of carbon implanted silicon layers for the orientation of the substrate (100) and (111).

In Fig.8 the half-width of the TO-phonon peak of SiC at perpendicular incidence of IR radiation on sample surface for spectra shown in Figs.2 (curve 1 – for substrate Si(100)) and 3 (curve 1' – for substrate Si(111)), versus an annealing temperature, is presented. The analogous dependences have been presented in previous papers [8, 47, 26]. However, the temperature range was narrower and, therefore, the maxima at 1200 and 1350°C were not found.

To explain these effects let us consider the ideal case again. We assume that the broadening of the absorption band due to different processes is absent and, therefore each frequency in the transmission spectrum corresponds to one or other bond between the atoms of the implanted layer. On this basis, we can see that, immediately after the implantation the contour of the transmission curve covers a wide range of frequencies, i. e. in ion-implanted layer



there are many different bonds that absorb at different frequencies. If one attributes the frequency of  $800\text{ cm}^{-1}$  to the tetrahedral oriented Si-C-bond of length of  $0.194\text{ nm}$  (bond characteristic of the silicon carbide), so in the implanted layer there are the systems with the bond lengths of both larger and smaller than this. In general, the presence of different bond lengths between the atoms of the ion-implanted layer is completely natural because atoms can stop at different distances from each other in the process of implantation.

In our case, the most interesting bonds are the single-, double- and triple silicon-silicon (Si-Si, Si=Si, Si≡Si), silicon-carbon (Si-C, Si=C, Si≡C) and carbon-carbon (C-C, C=C, C≡C) bonds presented in Fig.9. Simple covalent bond C-C, formed by the overlap of two  $sp^3$ -hybrid electron clouds along the line connecting the centers of atoms, is  $\sigma$ -bond. One of the electron pairs in the double C=C bond forms  $\sigma$ -bond, and the second bond is formed by p-electrons with the clouds in the form of "eight", which overlapping, form a  $\pi$ -bond. Triple C≡C bond is a combination of one  $\sigma$ -bond and two  $\pi$ -bonds [22]. The lengths of single bonds are shown in proportion to ones which are characteristic for these bonds in a tetrahedral orientation, although they can have various values in the ion implanted layer. And in the case of double and triple bonds they may be either higher or lower than the values given. The length of a single bond of the same type of atoms was taken equal to twice the covalent radius of atoms, and the length of the Si-C-bond was taken as half the sum of double the values of covalent radii of Si- and C without correction for their ionicity. The lengths of double and triple bonds were taken at  $0.021$  and  $0.034\text{ nm}$  shorter than a single bond, respectively. Triple bond between two atoms can be represented by two tetrahedra sharing a common face, and for the double bond - by two tetrahedra sharing a common edge [44].

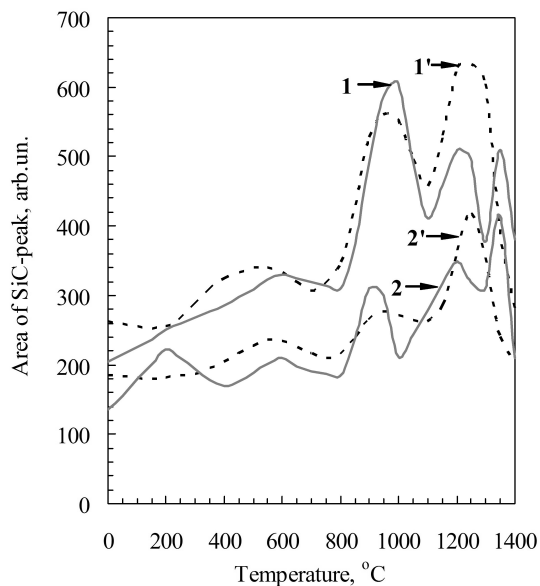


**Figure 6.** An area of the IR transmission peak for TO-phonons of SiC at perpendicular incidence of the radiation on the sample surface (curves 1, 1') and at  $73^\circ$  from a normal (curves 2, 2') for spectra presented in Figs.2 (curves 1, 2 - substrate Si(100)) and 3 (curves 1', 2' - substrate Si(111)), versus an annealing temperature.

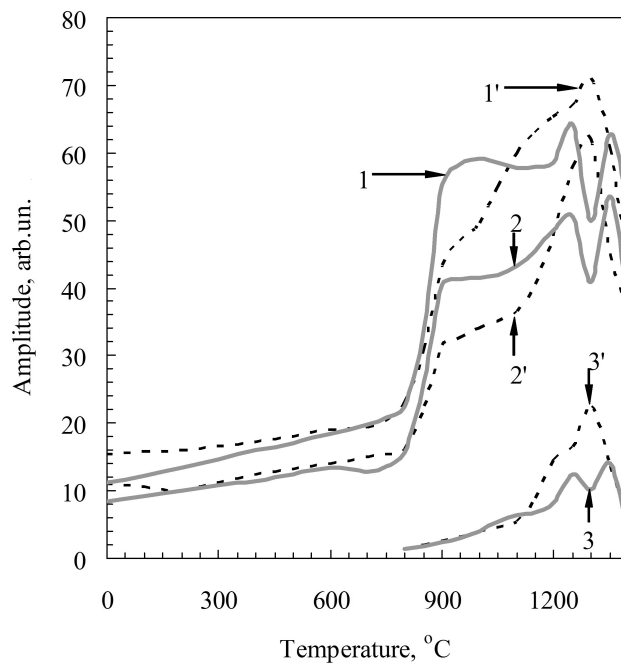


**Figure 7.** The IR transmission amplitude values for TO-phonons of SiC (curves 1, 1', 2, 2') at  $800\text{ cm}^{-1}$  and for LO-phonons of SiC (curves 3, 3') at perpendicular incidence of the radiation on the sample surface (curves 1, 1') and at  $73^\circ$  from a normal (curves 2, 2', 3, 3') to surface for spectra presented in Figs.2 (curves 1, 2, 3 - substrate Si(100)) and 3 (curves 1', 2', 3' - substrate Si(111)), versus an annealing temperature.

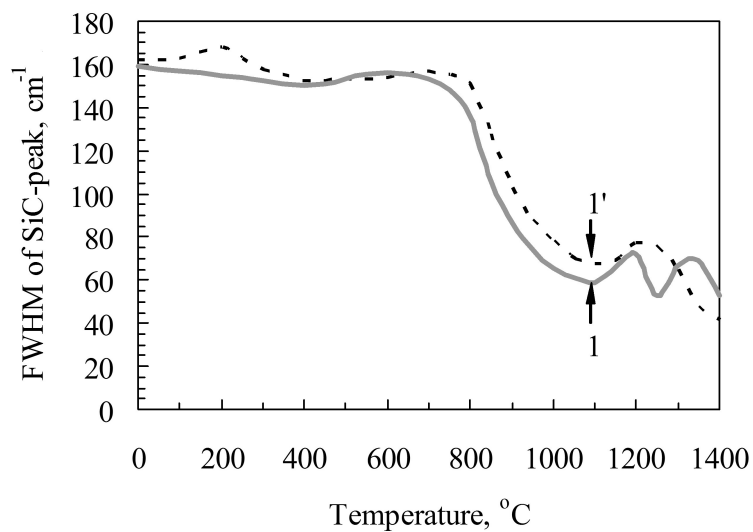


**Figure 8.** Half-width of the TO-phonon peak of SiC at perpendicular incidence of IR radiation on sample surface for spectra presented in Figs.2 (curve 1 – substrate Si(100)) and 3 (curve 1' – substrate Si(111)), versus an annealing temperature.

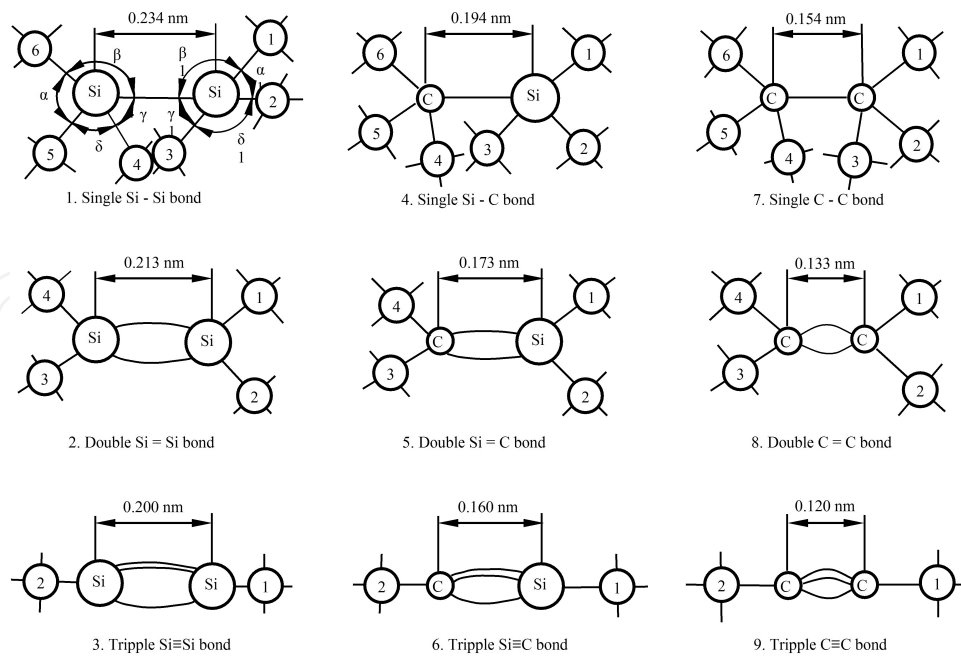


**Figure 9.** Various types of bonds between silicon, carbon atoms or their combination.

In the process of implantation of carbon into silicon vast majority of the covalent bonds of the substrate, starting with the amorphization threshold, are not covalent, because of violation of bond lengths and angles between them. However, among the formed Si-C-bonds there are tetrahedral bonds, the distances and angles between atoms of which correspond exactly to the crystallites of silicon carbide. This is confirmed by the presence of absorption at  $800\text{ cm}^{-1}$  and by the results of the authors [26] who identified by electron diffraction the presence of silicon carbide crystallites immediately after the implantation of carbon into silicon.

We believe that the ion-implanted layer consists mainly of various combinations of the nine types of bonds, shown in Fig. 9. Moreover, it is possible the presence in the implanted layer of the single elongated bonds, sesqui, free ("dangling") and hybridized bonds, as well as resonances and other higher order interactions as well. By making these assumptions, we proceed not only from the contour of the spectrum of infrared transmission, covering a wide range of frequencies. We are basing also on the ability of carbon and silicon atoms to form besides single bonds also double and triple bonds [29, 44, 64, 46]. In paper [27], an aggregate of carbon atoms was named as a cluster. In this paper, as a cluster we have in mind all the nine types of bonds and combinations thereof, from which are formed during annealing a three-dimensional clusters and crystallites of Si and SiC.

Table 1 presents the values of the binding energy for all nine types of bonds, shown in Figure 9. The sum of the energies of two and three single C-C bonds are equal to  $688$  and  $1032\text{ kJ mole}^{-1}$ , respectively, such that by  $73$  and  $220\text{ kJ mole}^{-1}$  higher than energy values of the C=C and C≡C bonds listed in Table 1. This suggests that the structures of the C=C and C≡C bonds for one bond has less energy than the structures with a single C-C bonds.

Types of bond	Binding energy, kJ mole <sup>-1</sup>	Types of bond	Binding energy, kJ•mole <sup>-1</sup>	Types of bond	Binding energy, kJ•mole <sup>-1</sup>
Si-Si	187	Si-C	290	C-C	344
Si=Si	<374	Si=C	<580	C=C	615
Si≡Si	<561	Si≡C	<870	C≡C	812

**Table 1.** The values of binding energy for nine types of bond.

By analogy, reasonable to assume that clusters Si=Si, Si≡Si, Si=C, Si≡C per bond also has less energy than clusters with single Si-Si and Si-C bonds. Consequently, the energy of double and triple bonds Si=C, Si=Si, Si≡C and Si≡Si must be less than the sum of the energies of two or three single Si-Si and Si-C bonds, as is shown in Table 1. It is evident that the most strongly bonds are the carbon-carbon and then carbon-silicon and silicon-silicon clusters.

Let us consider the special features of the curves on Figs.6–8 basing on the assumptions presented above.

*The temperature range 20-600°C*

It is known [65] that a typical recrystallization temperature of amorphous silicon lies in the temperature range 500–600°C. When the dose of the implanted carbon ions is much higher than the amorphization threshold and, the implanted atoms combining with the silicon atoms can form the inclusions of new compounds of considerable volume, the crystallization of silicon, in the case of a Gaussian distribution profile of implanted atoms, starts at the surface and the interface "disturbed layer – substrate" and goes in the direction to the maximum of the carbon distribution with increasing annealing temperature. The silicon crystallites are formed in regions where the concentration of silicon atoms exceeds the concentration of carbon.

The values of concentration ratio  $N_C/N_{Si}$  (Fig.1) are small on the edges of distribution and, a significant number of silicon atoms falls at each implanted carbon atom. In this temperature range, such combinations of clusters in ion-implanted layer are decaying which consist mainly of bonds of Si-Si, Si=Si and elongated Si-C, as they have the lowest energy dissociation among the types of bonds listed above. As decay of the clusters, we mean such regrouping of the atoms in system and the change the lengths of chemical bonds and angles between them, which lead to the most energetically favorable state of system. In such state there is a system of atoms with tetrahedrally oriented bonds, which are the most stable and durable. All other types of bonds and their geometrical arrangements are energy unprofitable; they are insufficiently stable and can decay during annealing.

As it is seen from curves 1 and 1' in the Figs. 6 and 7, the increasing of both an area of SiC-peak of IR transmission and its amplitude at 800 cm<sup>-1</sup> takes place over the temperature range 20–600°C, i.e. the formation of SiC crystallites takes place at temperatures significantly less that it is necessary for the SiC formation by a thermal growth. The mechanism of this phenomenon is of interest.

In the system "implanted layer – substrate", the phonons are generated in the process of annealing. This system is a single entity and, it is reasonable to assume that between the implanted layer and the substrate there is a continuous interaction of phonons. Since the thickness of the substrate is much greater than the thickness of the implanted layer, then, with respect to the layer, the substrate can act as a huge reservoir of phonons, which able, due to its heat capacity, receive or deliver the phonons to the implanted layer. As the implanted layer is thermodynamically nonequilibrium system, the process of interaction of phonons with the atoms will go towards reducing the free energy of the system. During each collision of a phonon with cluster of the implanted layer, the phonon absorption will occur if the energy of the system will decrease.

Energy released during the decay of clusters, is transferred to the lattice, which can accumulate and transfer it to another cluster, followed by the formation of energetically favorable system, in this case, the crystallites of Si and SiC. It is also possible direct transfer of energy of the decaying Si–Si-cluster to other types of clusters. In this temperature range, mainly, weakly bound Si–Si-clusters can decay during the interaction with phonons. More energy requires for the formation of crystallites of Si and SiC. This energy is transferred to the reacting atoms by the lattice. The considered above mechanism of formation of crystallites of Si and SiC, the so-called over-barrier mechanism, when the interacting atoms overcome the energy barrier of height  $E \cong E_{tr}$  is shown in Fig.10. This mechanism of formation of tetrahedrally oriented bonds Si–Si and Si–C from an energy point of view is advantageous for the crystal lattice, since it thereby reduces its free energy.

All possible mechanisms of the tetrahedral oriented Si–Si- and Si–C-bonds formation should be energy profitable for the crystalline lattice to decrease free energy of system. The formation of crystallites of Si and SiC in the range 20–600°C occurs mainly due to the decay of clusters such as the longest Si–Si- and Si–C-bonds, but also partly due to the disintegration of other types of clusters. A number of studies have shown [5, 26], that immediately after the implantation, the presence of a minute quantity of SiC crystallites with hexagonal structure is observed in the ion implanted layer and, they are transformed into  $\beta$ -SiC at the temperature of 400°C and higher. It is impossible to identify the presence of Si crystallites due to their optical inactivity in this range of the infrared absorption. However, their presence is not in doubt, as much less energy is required to expend for their formation than for the formation of SiC crystallites at the implementation of over-barrier mechanism. As we showed earlier, in layers SiC<sub>0.03</sub> with a low carbon concentration the crystallites of Si increase their sizes from 2 to 3 nm in the range 20–700°C (Fig.11).



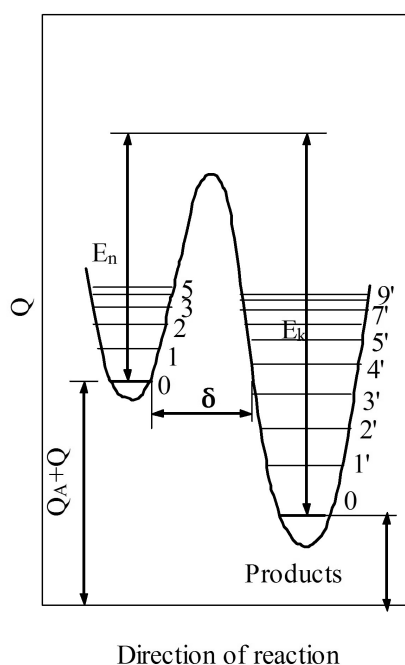


**Figure 10.** Illustration of the over-barrier mechanism of the formation of the tetrahedral oriented bonds

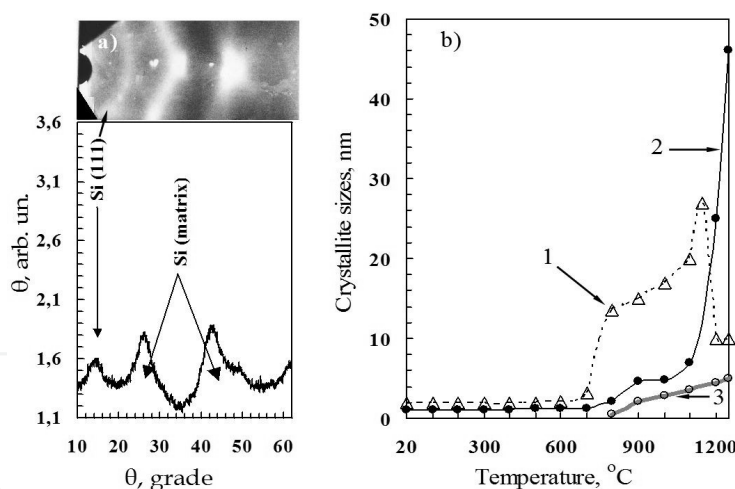


**Figure 11.** X-ray diffraction patterns of the  $\text{SiC}_{0.12}$  layer after implantation (a) and average sizes of crystallites in the (111) plane after implantation and annealing (b): 1 – Si (for layer  $\text{SiC}_{0.03}$ ), 2 – Si (for layer  $\text{SiC}_{0.12}$ ), 3 – SiC (for layer  $\text{SiC}_{0.12}$ ).

Peak area immediately after implantation is not zero, i. e. a part of the carbon atoms is included into composition of the optically active clusters (Fig.6). If we assume that, after annealing at 1000-1250°C almost all carbon atoms are optically active and optically inactive clusters broke up, we see that immediately after the implantation of carbon into the (100) and (111) oriented silicon at least 65% and 60% of carbon atoms were concentrated in optically inactive clusters, respectively, if the implantation was carried out by a dose sufficient to obtain the stoichiometric concentration ( $E = 40 \text{ keV}$ ,  $D = 3.56 \times 10^{17} \text{ cm}^{-2}$ ). A number of carbon atoms is included into

stable types of optically inactive clusters which stable up to melting point of silicon. It is known [44], that the optically inactive objects consist of the clusters and their chains that lie in one plane. The formation of clusters and chains of planar systems of nets may be due to energy considerations. For example, in [5] the formation of alternating layers of single crystal silicon with amorphous silicon precipitates enriched with carbon in the ion-implanted layer, attributed to the fact that the system in such a way reduces its free energy.

Spatial pattern of ion-implanted layer is difficult to model, since a Gaussian distribution profile of implanted atoms is characterized by the change by depth of the concentration of carbon atoms  $N_C/N_{Si}$  and, thus, the mechanism of physical processes from one layer to layer is changed. We can construct a flat infrared inactive net in the middle of layer where  $N_C/N_{Si} = 1$ . Flat optical inactive net consisting of C and Si atoms, linked by single, double and triple bonds, may also contain free ("dangling") bonds of the silicon and carbon atoms. These bonds may connect to atoms of the other flat net or on the association of the atoms which do not lie in one plane. The atoms which do not lie in one plane, can form an association of optically active clusters.

With increasing annealing temperature at first the decay of elongated single bonds at two atoms united by a triple bond, is taken place. These pairs of atoms inhibit the diffusion of atoms in the layer. Then, the energetically unfavorable single bonds of atoms are disintegrated in the planar nets of clusters. The subsequent increase in annealing temperature would lead to the disintegration of the planar nets forming a number free carbon and silicon atoms, as well as pairs of Si and C atoms, linked together by multiple bonds. Free carbon and silicon atoms can move on short distances and join to form the crystallite Si or SiC, which is profitable from an energy point of view and, as a result, the energy of system is decreased.

In addition to the planar nets of clusters, the ion-implanted layer may contain long chains of clusters, which are also optically inactive. The chains can be formed by alternating different types of bonds, and their degradation temperature may be different. There are also local clusters non-interacting with the surrounding atoms and consisting of three-, four- and more atoms linked together by double bonds. They are most stable clusters due to the full richness of their bonds. Perhaps these clusters are not disintegrated up to the melting point of layer.

In Fig.12 the IR transmission amplitude versus the annealing temperature for different frequencies is shown. It is evident that clusters absorbing at frequencies of 850 and 900  $\text{cm}^{-1}$ , in the range 20–600°C did not disintegrated, as their amplitude remains unchanged. The position of minimum of IR transmission peak does not change and is located at 757  $\text{cm}^{-1}$  (Fig.4). This indicates the dominant role of one type of clusters, which absorb at 757  $\text{cm}^{-1}$ . The increase of the amplitude of the peak (Fig. 12, curve 3) indicates an increase in the concentration of these clusters with increasing annealing temperature. At the same time the concentration of clusters, which absorb at 700  $\text{cm}^{-1}$  and correspond to the elongated single bond, is simultaneously increased. The energy of both the formation and decay of these bonds is a least one ( $E = h\nu$ ), as they absorb the radiation of lowest frequencies among considered. It follows from Fig.7 (curve 1) and 12 (curve 1), that the bonds being very similar to tetrahedral bonds of SiC which absorbs at 800  $\text{cm}^{-1}$ , are formed in the implanted layer. That

follows also from decrease of peak halfwidth (Fig.8) in temperature range 20–400°C. Its increase in range 400–600°C may be associated with intensive restructuring of Si–Si bonds of amorphous silicon before recrystallization at the surface and near the substrate, where the concentration of carbon is low. The increase in peak area of the TO-phonon SiC in this range (Fig. 6, curves 1, 1') is caused by an increase in the number of tetrahedral bonds and close to them, which absorbs in the range 750–850 cm<sup>-1</sup> (Fig.12, curves 1, 3, 5).

No significant differences between the properties of the films on the substrate orientation (100) and (111) in this temperature range were observed, except for the fact that the area of SiC-peak and amplitude at 800 cm<sup>-1</sup> are slightly higher for the orientation (111), which indicates a higher number of tetrahedral bonds of SiC and a smaller number of optically inactive clusters.

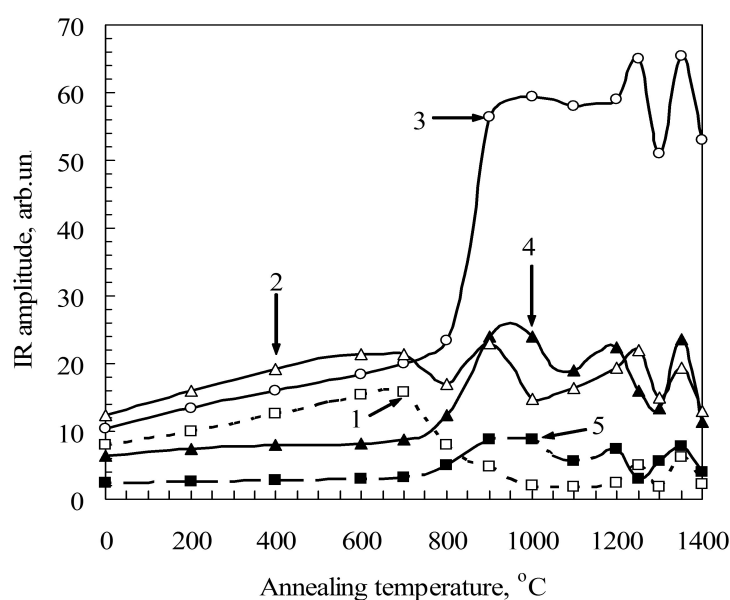


**Figure 12.** Amplitude of IR transmission for various wavenumber values versus an annealing temperature. (1 - □) 700 cm<sup>-1</sup>, (2 - Δ) 750 cm<sup>-1</sup>, (3 - ○) 800 cm<sup>-1</sup>, (4 - ▲) 850 cm<sup>-1</sup>, and (5 - ■) 900 cm<sup>-1</sup>.

#### *The temperature range 600–800°C*

The area under IR spectrum curve is decreased in this temperature range (Fig.6) due to the decay of the optical active clusters absorbing at the frequencies close to 700 and 750 cm<sup>-1</sup> (Fig.12). As shown in previous studies (Fig. 13d, e), this is due to the decay of elongated Si–C-bonds in the layers with a low concentration of carbon. An intensive process of disintegration of these bonds occurs in layers SiC<sub>0.4</sub> and SiC<sub>0.12</sub> between the surface and the maximum of the carbon distribution. In addition of the decay of the optical active non-tetrahedral Si–C-bonds, seemingly, deformed Si–Si bonds are disintegrated, too.

The intensive rearrangement of clusters is characterized for this temperature range. As a result of multiple collisions the atoms of clusters, successively passing from the initial-through the intermediate states to the most energy favorable end position, form the tetrahedrally oriented bonds of Si- and SiC crystallites. A significant change of halfwidth of

the Si-C-peak of IR spectrum begins for film on (100) oriented substrate (Fig.8). In case of (111) oriented silicon substrate the same is taken place some later. A certain increase of the concentration of clusters absorbing on the wavenumbers ranged from 850 to 900  $\text{cm}^{-1}$  (Fig. 12, curves 4, 5) is simultaneously taken place. The ordering of layer structure in region near the substrate is taken place, too.

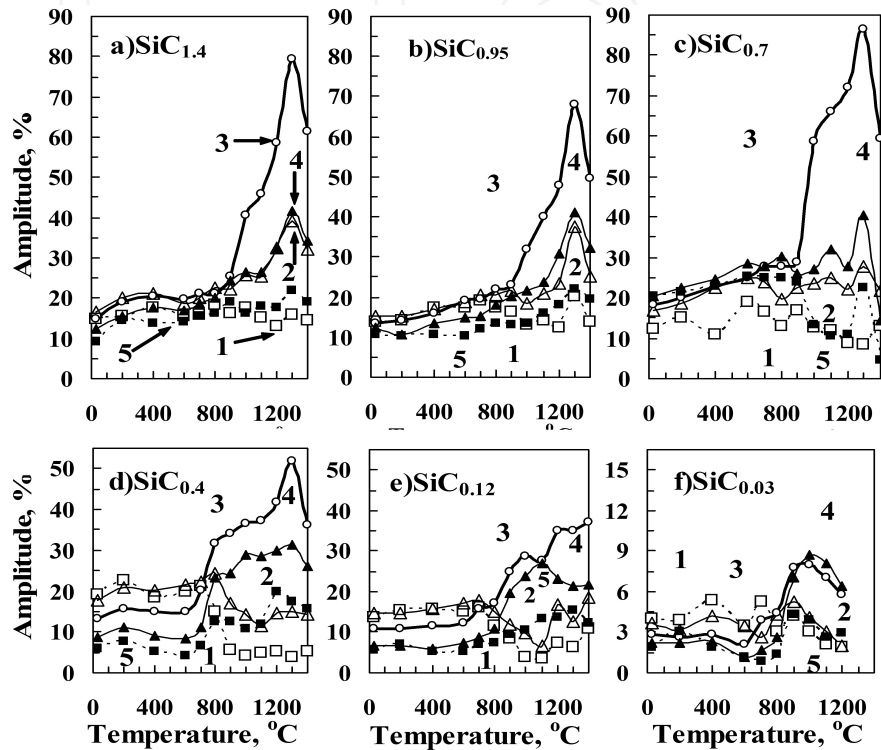


**Figure 13.** Effect of the annealing temperature on the IR transmission amplitude at wavenumbers of (1-□) 700  $\text{cm}^{-1}$ , (2-△) 750  $\text{cm}^{-1}$ , (3-○) 800  $\text{cm}^{-1}$ , (4-▲) 850  $\text{cm}^{-1}$ , and (5-■) 900  $\text{cm}^{-1}$  under normal incidence of IR radiation on the sample surface: a)  $\text{SiC}_{1.4}$ ; b)  $\text{SiC}_{0.95}$ ; c)  $\text{SiC}_{0.7}$ ; d)  $\text{SiC}_{0.4}$ ; e)  $\text{SiC}_{0.12}$ ; f)  $\text{SiC}_{0.03}$ .

#### *The temperature range 800-1000°C*

Accordingly to Figs. 6-8 and 12 almost whole ion implanted layer takes place in the process of crystallization of Si and SiC in this temperature range. The probability of over-barrier mechanism of the formation of Si- and SiC crystallites, seemingly, is increased as is seen from the significant increase of the IR transmission amplitude at 800  $\text{cm}^{-1}$  (Fig.7, curves 1, 1'). The flat net of clusters and the chains of them in a great extent are disintegrated. The intensive decay of the infrared active non-tetrahedral Si-C-bonds is taken place and, the sesquiteral- and, partially, the double silicon-silicon bonds simultaneously with the infrared inactive single bonds can disintegrated as well. Seemingly, the energy of the phonons may be sufficient for the disintegration of the infrared inactive C-Si-, C-C- and even C=Si-bonds. Simultaneously, the formation of the most energy favorable tetrahedrally oriented bonds of Si- and SiC-crystallites is taken place (Figs. 6, 7, curves 1, 1'; Fig.12, curve 3). The continuous process of the formation of the infrared active clusters absorbing on the frequencies close to

700–800  $\text{cm}^{-1}$  is taken place in the layer and, the concentration of these clusters with the increasing of the annealing temperature is increased. The absorption at 800  $\text{cm}^{-1}$  begins significantly predominate over the ones at another frequencies. That leads to the significant increase of the IR transmission amplitude at this frequency in comparison with the increase of amplitude at another ones (Fig.12, curve 3) and, that is perceived as a frequency shift of the IR absorption maximum (Fig.4). The increase of concentration of clusters absorbing on frequencies higher than 800  $\text{cm}^{-1}$  is observed, too (Fig. 12, curves 4, 5).

So, the increase of the area under the IR transmission curve in the temperature range 800-1000°C is caused, mainly, by the absorption at frequency of 800  $\text{cm}^{-1}$ , i.e. by bonds characteristic to the SiC-crystallites and, by bonds absorbing on frequencies both more and less than 800  $\text{cm}^{-1}$  as well. In the case of the (100) oriented substrate the number of tetrahedral Si–C-bonds reached at 1000°C some maximum and does not change up to 1200°C, whereas in the case of orientation (111) it increases going smoothly in the range 900-1300°C. Comparison with the data in Fig.13 shows that such flat areas of curves at these temperatures are typical for the layers  $\text{SiC}_{0.7}$ , and especially for  $\text{SiC}_{0.4}$ . The total dose of implanted ions of carbon in the case of  $\text{SiC}_{0.7}$  was  $D(\text{SiC}_{0.7}) = 4.54 \times 10^{17} \text{ cm}^{-2}$ , and  $D(\text{SiC}_{0.4}) = 2.72 \times 10^{17} \text{ cm}^{-2}$ , and is comparable to the dose of carbon ions with an energy of 40 keV for the considered Gaussian distribution of carbon:  $D(40 \text{ keV}) = 3.56 \times 10^{17} \text{ cm}^{-2}$ . The halfwidth of IR-spectrum maximum (Fig.8) in the range 800-1000°C is rapidly decreased. That is an evidence of a significant ordering of the ion implanted layer structure caused by the formation of Si- and SiC-crystallites. It goes more intensively in case of (100) orientation of substrate.

#### *The temperature range 1000-1100°C*

In spite of the fact that the formation of new SiC crystallites in the implanted layer at these temperatures is not taken place (Fig.7, curve 1, 1'; Fig.12 and 16, curves 3), the decrease of area of SiC-peak of IR transmission curve is significant (Fig.6, curves 1, 1'). As it was shown earlier (Fig.11), the dimensions of Si- and SiC-crystallites are enlarged with the increase of the annealing temperature. Thereby, we believe that in this temperature range the uniting of small crystallites of Si and SiC in the larger ones is taken place, resulting the frequency shift of LO-phonon peak in IR spectrum to a higher frequency (Fig. 4), as well as the growth of its amplitude (Fig. 7, curve 3). When combining the crystallites, in the area of their union the decay of the both optically active and inactive clusters is taken place. This explains the decrease in the amplitude of the infrared transmittance for clusters absorbing at frequencies of 800-900  $\text{cm}^{-1}$  (Fig. 12) and the corresponding decrease in the area (Fig. 6). Apparently, this temperature is insufficient for the decay of clusters C=Si and C=C and, as a result the formation of new SiC crystallites is not observed. However, a volume of polycrystalline Si is continuously increased due to the disintegration of Si-Si, Si=Si bonds in regions with low concentration of carbon (Fig.1, regions I and II).

In the case of the substrate orientation Si(111), the SiC-peak area is reduced to a lesser extent, and is larger after annealing at 1100°C than the peak area for the substrate Si(100) due to the fact that the number of tetrahedral bonds and crystallites continues to grow.

#### *The temperature range 1100-1200°C*



Both the area of Si–C-peak (Fig. 6) and its half-width (Fig. 8) increase in this temperature interval, while the volume of the polycrystalline SiC is unchanged (Fig. 12, curve 3 and Fig. 7, curve 1), as the further growth of SiC crystallite size due to their association (Fig. 4, curves of LO-phonons) is taken place. The growth of the area and half-width of Si–C-peak are caused by the formation of new optically active clusters absorbing at frequencies of 750-900  $\text{cm}^{-1}$  (Fig. 12) due to the decay of stable clusters. As a result, the ion-implanted layer degrades the structure (increase in half-width of the peak).

*The temperature range 1200-1250°C*

No significant changes in the formation of new infrared active clusters over this range are taken place. The decaying clusters with short Si–C-bonds, absorbing at frequencies of 800–900  $\text{cm}^{-1}$  (Fig. 12, curves 1-3) are converted into clusters with long bonds, absorbing at 700 and 800  $\text{cm}^{-1}$  (Fig. 12, curves 4 and 5). Therefore, the area of Si–C-peak is not changed (Fig.6) for both orientations of substrate (100) and (111). The annealing temperature 1250°C may be sufficient for the decay of sesqui- and double Si–C-bonds. As a result, the concentration of tetrahedrally oriented Si–C-bonds increases, the atoms are combined into crystallites of SiC, and the amplitude of the IR spectrum at 800  $\text{cm}^{-1}$  increases (Fig. 12, curve 3). There is a further streamlining of the structure of the ion-implanted layer (Fig. 8), both due to the formation of new crystallites of SiC, as well as due to an increase in their size (Fig. 4, curve of LO-phonons).

*The temperature range 1250-1300°C*

Seemingly, there may be competing processes here. Firstly, in the case of the substrate Si(100) in this interval there is a decay of a large number of tetrahedral bonds (Fig. 7, curve 1), which is the main reason for reducing the area of SiC-peak at 1300°C (Fig. 6, curve 1). At the same time the amplitude of the LO-phonon is decreased (Fig. 7, curve 3) and the half-width of the peak is increased (Fig. 8, curve 1), indicating a deterioration of the structure. In contrast, in the case of the substrate Si(111) the peak area (Fig. 6, curve 1') and the amplitude at 800  $\text{cm}^{-1}$  (Fig. 7, curve 1') are increased, and this is accompanied by a decrease in the half-width of the TO-phonon peak and an increase in amplitude of the LO-phonon peak (Fig. 7, curve 3'), i.e. by the improving of the layer structure. We assume that there may be two dominant mechanism of the influence of substrate orientation on the layer structure at high temperatures. During the recrystallization of the damaged layer in the interface "the SiC film – Si substrate", both a destruction of the silicon crystallites and the uniting of their atoms with the substrate are taken place. The difference of the recrystallization of the substrate Si(100) may be the appearance of forces and conditions for the destruction of the defective crystallites of silicon carbide. This leads to a decrease in amplitude at 800  $\text{cm}^{-1}$  and increase the half-width of the peak due to the appearance of non-tetrahedral Si–C-bonds. The second mechanism may be associated with different concentrations of carbon near the surface of silicon. After implantation into (100) oriented Si substrate, the carbon-riched surface layer is much thicker than in case of Si(111) substrate, so the sublimation and desorption of carbon at high temperatures will lead to a significant decrease in the amplitude values of the SiC-peak at all frequencies. Ie, the experiments to study an influence of substrate orientation on the desorption of implanted carbon are necessary.

*The temperature range 1300-1350°C*

Despite the increase in the desorption of carbon, the area of SiC-peak (Fig. 6), as well as the amplitude at all frequencies of spectra are increased in case of the film on the substrate Si(100) (Fig. 12, curves 1-5). The atoms of clusters, which formed due to the destruction of defective crystallites of SiC in the previous temperature range, re-unite again in form of the crystallites of SiC, as well as in form of optically active clusters, which absorb at frequencies near  $800\text{ cm}^{-1}$ . In addition, stable clusters with Si=C, Si $\equiv$ C and C=C bonds are disintegrated (Fig. 9). Growth of SiC crystallite size leads to a frequency shift of LO-phonons peak in the short-wavelength region (Fig. 4). Since in an isolated system unacceptable the processes occurring with increasing free energy, the uniting of two crystallites occurs, if is accompanied by a gain in energy in comparison with the energy expended in their decay. In the case of the orientation of the substrate Si(111) a decrease of the area of SiC-peak (Fig. 6, curve 1'), as well as the amplitude at  $800\text{ cm}^{-1}$  (Fig. 7, curve 1') occur due to increased desorption of carbon.

*The temperature range 1350-1400°C*

Although at these temperatures the decay of optically inactive clusters, formation of both new crystallites and optically active SiC-clusters should be the greatest, nevertheless the growth of area and the amplitude of the SiC-peak of IR spectrum is not observed. On the contrary, they decrease (Fig. 6 and 7), which can be explained to the dominant influence of sublimation and desorption of carbon. The volume of polycrystalline SiC is also reduced, which is accompanied by a decrease in the amplitude of LO-phonons (Fig. 7, curve 3). A further ordering of the structure of ion-implanted layer occurs, as evidenced by the decrease in the peak half-width of IR spectrum.

In conclusion, it is necessary to note that the quantity of absorbing Si-C-bonds in the silicon layer with Gaussian distribution of implanted carbon reaches a maximum at  $1000^\circ\text{C}$  for (100) oriented substrate and, at  $1000$  and  $1250^\circ\text{C}$  for (111) oriented substrate (Fig. 6). Most of the carbon atoms combine with atoms of silicon, forming the tetrahedrally oriented bonds of SiC (Fig. 12, curve 3). Seemingly, there are flat nets and chains of clusters (Fig. 9), which consist mainly of bonds Si-Si, Si = Si, C-Si, C-C and, this temperature is sufficient for their decay. Some significant part of the carbon atoms form bonds of higher order, which decay at temperatures of  $1200$ - $1400^\circ\text{C}$  and above. At high temperatures,  $1300$ - $1400^\circ\text{C}$  (Figs. 6 and 7) occur intense desorption processes of carbon.

*A shape of IR transmission peak*

All presented spectra (Fig.2) have shape different from simply dispersive spectrum (theoretically calculated). The transmission band both left and right from the transmission peak are perceptible asymmetric and, one can not describe it's shape by a simple analytical function. The shape asymmetry is decreased with the annealing temperature increasing and, it is minimal in the temperature range  $1300$ - $1350^\circ\text{C}$ . The further increase of the annealing temperature leads to the increase of asymmetry, too. The contour of the transmission peak for TO-phonons at perpendicular incidence of electromagnetic radiation on sample surface after annealing at  $1350^\circ\text{C}$  is most close to the dispersive one.

Obviously, the asymmetry of IR transmission contour is related with the presence of the infrared active clusters in the ion implanted layer, and the concentration of clusters is minimal when the asymmetry is minimal, i.e. at 1350°C. In this relation, a largest area of SiC-peak corresponds to maximum amplitude of absorption at wavenumber 800 cm<sup>-1</sup> (Figs.7 and 8). As is seen from amplitude values in Fig.12 (curves 1, 2, 4, 5), there is a certain quantity of the non-tetrahedral optical active clusters at 1350°C. Seemingly, a presence of very stable optical inactive clusters, which are not disintegrated even at the melting point of Si, is possible.

#### *Measurement of a conduction type of carbon implanted silicon layer*

The (100) oriented substrates of n- and p-Si of dimensions 7×5×0.3 mm<sup>3</sup> with resistivities 4–5 Ом см have been implanted by carbon ions with values of energy 40 keV and dose 3.56×10<sup>17</sup> cm<sup>-2</sup> to determine a type of conduction. After implantation, the samples have been isochronously annealed in vacuum over the temperature range from 200 up to 1200°C with step 200°C for 30 min. A surface layer of the annealed samples have been removed by etching in an acid mixture HF:HNO<sub>3</sub> in composition of 1:10. A type of conduction of the implanted surface has been determined using thermo-emf after each 0.5 mm along both horizontal and vertical directions. The thermo-emf have fixed with approximately equiprobability the both n- and p-type of conduction on n-Si substrates, while on the p-Si substrates the thermo-emf have shown the p-type of conduction only. We believe that p-type of conduction on the n-Si substrates is provided by the SiC crystallites. The conduction of the Si crystallites is similar to the conduction of the substrate. If the substrate is p-Si, so the both Si- and SiC-crystallites have the p-type of conduction. So, the synthesized SiC-crystallites have p-type of conduction independently from the type of substrate.

### **3.2. Investigation of high-temperature instability of solid SiC films synthesized by ion implantation**

As stated in paragraph 2, for construction of a rectangular profile of the distribution of carbon atoms in the silicon, the implantation of carbon ions of different energies and doses in the second group of single-crystal silicon wafers of n- and p-type conductivity was carried out sequentially in the order according to Table 2. The doses of ions were chosen in such a way to obtain a layer SiC<sub>0.7</sub> with the ratio of the concentrations of carbon and silicon atoms through a depth of about  $N_C/N_{Si} = 0.7$ . Postimplantation annealing of the samples was performed in a vacuum in the temperature range 200-1200°C for 30 min with a step 200°C. In some cases, to compare also were analyzed the samples with films SiC<sub>0.95</sub>.

E, keV		40	20	10	5	3
D(SiC <sub>0.7</sub> ), 10 <sup>17</sup> cm <sup>-2</sup>		2.80	0.96	0.495	0.165	0.115
D(SiC <sub>0.95</sub> ), 10 <sup>17</sup> cm <sup>-2</sup>		4.48	1.54	0.792	0.264	0.184
N <sub>C</sub> (Gibbons) profile [21]	R <sub>p</sub> (E), nm	93.0	47.0	24.0	12.3	7.5
	ΔR <sub>p</sub> (E), nm	34.0	21.0	13.0	7.0	4.3

**Table 2.** Values of energy, E, dose, D, projected range, R<sub>p</sub>(E), and straggling, ΔR<sub>p</sub>(E), for <sup>12</sup>C<sup>+</sup> ions in Si, used for constructing a rectangular distribution profiles SiC<sub>0.7</sub> and SiC<sub>0.95</sub>.

### 3.2.1 Influences of annealing, sputtering and the film composition changes during high dose implantation on the thickness and shape of the distribution profile of carbon atoms

Fig. 14 shows the calculated profile  $N_C(\text{Gibbons})$  of distribution of carbon atoms through the depth of silicon for the energies and doses of ions according to Table 2, which is the sum of Gaussian distributions constructed with the use of  $R_p(E)$  and  $\Delta R_p(E)$  by [21] (LSS) in accordance with the expression:

$$N(x) = \frac{D}{\Delta R_p (2\pi)^{1/2}} \exp\left[-\frac{(x - R_p)^2}{2\Delta R_p^2}\right] \quad (5)$$

where  $x$  – the distance from the surface.

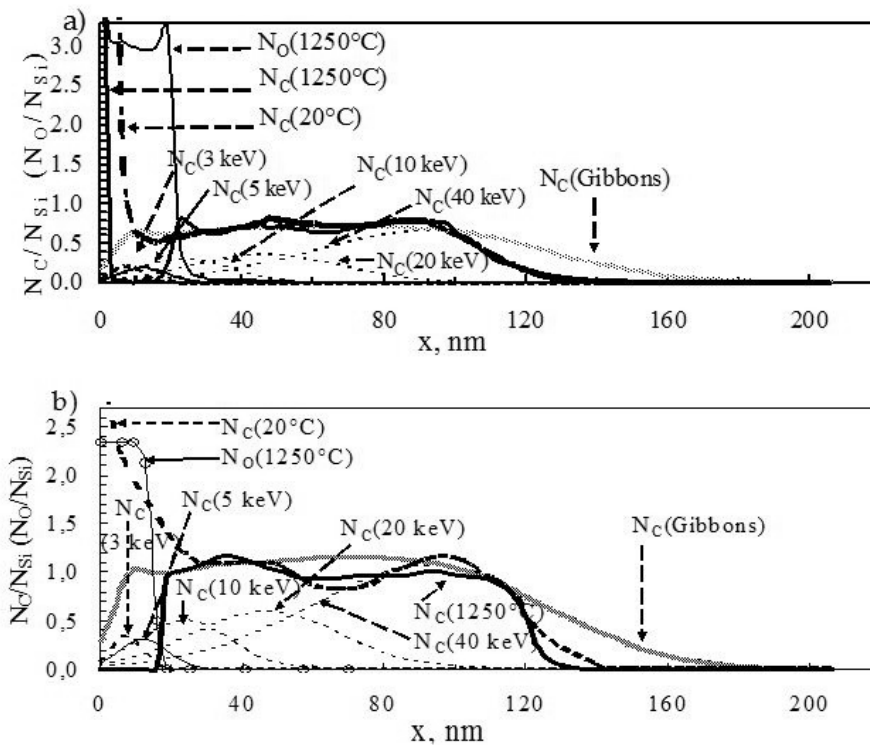


**Figure 14.** distribution profiles in Si produced by ion implantation (see Table 2). (a)  $\text{SiC}_{0.7}$ ; (b)  $\text{SiC}_{0.95}$ .  $N_C(\text{Gibbons})$  is the profiles calculated according to [21], where  $N_C(\text{Gibbons}) = N_C(40 \text{ keV}) + N_C(20 \text{ keV}) + N_C(10 \text{ keV}) + N_C(5 \text{ keV}) + N_C(3 \text{ keV})$ .  $N_C(20^\circ\text{C})$ ,  $N_C(1250^\circ\text{C})$  and  $N_O(1250^\circ\text{C})$  are the Auger profiles of carbon and oxygen, respectively, in a layer after high-dose implantation and annealing at  $1250^\circ\text{C}$  for 30 min.

Fig. 14 also shows the experimental curves (Fig. 14, curves  $N_C(20^\circ\text{C})$ ,  $N_C(1250^\circ\text{C})$  and  $N_O(1250^\circ\text{C})$ ), obtained by Auger electron spectroscopy, showing the ratio of the concentrations of carbon and oxygen atoms to silicon ( $N_C/N_{Si}$  и  $N_O/N_{Si}$ ) through the depth of the sample after implantation ( $20^\circ\text{C}$ ) and annealing at  $1250^\circ\text{C}$  for 30 min in an argon atmosphere containing some oxygen. These distributions are constructed through a depth, taking into account the condition that the number of carbon atoms in silicon and, consequently, the inte-



grals and the area under the curves  $N_C(\text{Gibbons})$  and  $N_C(20^\circ\text{C})$  must be equal one another at a first approximation. The areas under the curves were equal to  $S_G = S_{20^\circ\text{C}} = \int (N_C / N_{\text{Si}}) dx = 90$  units (or 100%), and after annealing at  $1250^\circ\text{C}$ :  $S_{1250^\circ\text{C}} = 71$  units (or 79.4%) due to the formation of silicon oxide layer. When evaluating the number of carbon atoms in a thin surface region (8 nm), where  $N_C/N_{\text{Si}}$  is very great due to the low content of silicon atoms ( $N_{\text{Si}} \ll 5 \times 10^{22} \text{ cm}^{-3}$ ), an approximation was made that the  $N_C/N_{\text{Si}}$  does not exceed 2.3 ( $N_{\text{graphite}} = 11.6 \times 10^{22} \text{ cm}^{-3}$  and  $N_{\text{silicon}} = 5 \times 10^{22} \text{ cm}^{-3}$ ). At the same time, the area under the profile curve for the region  $x > 22.2$  nm were estimated  $S_G = 78$  units,  $S_{20^\circ\text{C}} = 66$  units and  $S_{1250^\circ\text{C}} = 65$  units. That is, the areas under the profile curves before and after annealing for  $x > 22.2$  nm are almost equal, but less than calculated value, since part of the carbon atoms after implantation was concentrated near the surface ( $x < 8$  nm), and during annealing occur desorption of carbon from the layer ( $x < 22.2$  nm) and the formation of silicon oxide. The interface "the SiC film - Si substrate" in the experiment was more abrupt than it was expected. After annealing for 30 minutes, almost 20% of the total number of carbon atoms desorbed from the carbon-rich surface layer of the film. Fig. 14 shows that the average concentration of carbon and oxygen were:  $N_C/N_{\text{Si}} = 0.7$  in the depth  $22.2 < x < 110$  nm and the  $N_{\text{O}}/N_{\text{Si}} \approx 3.0$  at the surface layer  $x < 22.2$  nm. In this case there is penetration of oxygen atoms into the layer up to 30 nm.

Some difference between the shape of the experimental and calculated curves of the profile is observed (Fig. 14). The distribution  $N_C(\text{Gibbons})$  was made without taking into account the effects of sputtering and composition changes in the layer by high dose implantation. Accounting for the effect of surface sputtering during high dose of implantation of carbon ions ( $E = 40$  keV,  $D = 2.8 \times 10^{17} \text{ cm}^{-2}$ ) allows to assume the displacement of profile further into the layer with increasing dose, to some expansion of the profile and, consequently, to reduce the carbon concentration at the peak of the distribution in comparison with the calculated value. However, changing the composition of the single-crystal silicon substrate up to a mixture of C and Si atoms during the implantation suggests the formation of a significant amount of double and tripple Si-C- and C-C-bonds, which are more strong than the Si-Si-bonds, as well as the formation of stable carbon and carbon-silicon clusters. This results a decrease of  $R_p(E)$  and  $\Delta R_p(E)$  during implantation.

The decrease of  $R_p(E)$  decreases the influence of surface sputtering on the position of the distribution maximum of carbon atoms, i.e., the maximum should remain nearly on the same depth. Moreover, the decrease of  $\Delta R_p(E)$  will increase the carbon concentration at the maximum of peak and a more sharp decrease in concentration in the direction to the substrate and to the surface. This will cause a decrease in the depth of the interface "film SiC – the substrate Si», which becomes more sharp with increasing dose, as well as an occurrence of depression between peaks 40 and 20 keV, and possibly between 20 and 10 keV. The appearance of depression between peaks 40 and 20 keV in Fig. 14 for layers  $\text{SiC}_{0.7}$  and  $\text{SiC}_{0.95}$  may be due to these reasons.

The surface sputtering during the implantation of carbon ions with energies of 10, 5 and 3 keV is more intense with decreasing ion energy. This should lead to an increase in carbon concentration near the surface due to shift of the distribution maxima of these ions one to



another ( $N_C(3 \text{ keV})$  and  $N_C(5 \text{ keV})$  in the direction of  $N_C(10 \text{ keV})$ ). As a result, significant increase in the concentration of carbon in the surface layer is observed.

It is seen in Fig.14b that the average concentration of carbon and oxygen were:  $N_C/N_{Si} = 0.95$  in the depth of the layer from 20 to 110 nm and the  $N_O/N_{Si} \approx 2.33$  at the surface layer up to a depth of about 20 nm. At the same time observed the penetration of oxygen up to 80 nm to the depth. It was found for a layer  $SiC_{0.95}$  that  $S_G = S_{20^\circ C} = \int (N_C / N_{Si}) dx = 144$  units (or 100%), and after annealing at  $1250^\circ C$ :  $S_{1250^\circ C} = 103$  units (or 71.3%). Thus, it appears that after annealing for 30 minutes, almost 30% of the carbon atoms desorbed from the surface layer of the film. At the same time the appearance of a layer of oxygen atoms at the surface is revealed. The area under the profile curve for the region  $x > 25$  nm were estimated  $S_G = 121$  units,  $S_{20^\circ C} = 99$  units and  $S_{1250^\circ C} = 95$  units. i.e., the area under the curves of the profile before and after annealing for region  $x > 25$  nm are similar in magnitude, but again less than calculated one, since part of the carbon atoms after implantation was concentrated near the surface ( $x < 19$  nm), and after annealing, there was desorption of carbon from layer ( $x < 25$  nm) and the formation of silicon oxide. The interface "the SiC film – Si substrate" in the experiment also was sharper than the expected one.

The presence of a sharp interface "the SiC film – Si substrate" permits to suppose that is possible to obtain promising results on the measurement of film thickness by X-ray reflectometry, although this method is typically used for films deposited with a very sharp interface "a film - substrate" and for ion-implanted layers usually does not apply. The parameters of the  $SiC_{0.7}$  film by this method were investigated at small grazing angles  $\theta$  by recording the angular dependence of the reflection coefficient using two spectral lines  $CuK_\alpha$  (0.154 nm) and  $CuK_\beta$  (0.139 nm) on the installation "ComplexXRay C6" [61]. The oscillations of intensity were observed, assigned to the interference of X-ray reflections in the layers  $SiC_{0.7}$  and  $SiO_2$  (Fig. 15).

The first maximum of reflection with intensity  $I_1 = 93207$  pulses at an angle of  $2\theta = 0.418^\circ$  is observed (Fig. 15). The angle of total external reflection is evaluated as an angle where the intensity is equal to a half of the first maximum ( $I = I_1/2 = 46603$  pulses), ie  $2\theta_c = 0.449^\circ$ , or  $\theta_c = 0.2245^\circ = 3.918$  mrad. Using the Henke program is determined that this value of  $\theta_c$  corresponds to the value of film density  $2.37 \text{ g/cm}^3$ , which is close to the density of cristobalite ( $SiO_2$ )  $2.32 \text{ g/cm}^3$ . Further, with increasing of the incidence angle, the intensity of reflection increases again up to  $I_2 = 76831$  pulses and that indicates the presence of a more dense structure. If the intensity falls up to the value  $I = I_2/2 = 38415$  pulses, the value  $2\theta_c = 0.486^\circ$ , the critical angle is equal to  $\theta_c = 0.243^\circ = 4.241$  mrad, which corresponds to a density  $2.77 \text{ g/cm}^3$  and is close to the density of quartz ( $SiO_2$ )  $2.65 \text{ g/cm}^3$ . As shown in Fig. 15, then there is a second increase in intensity up to  $I_3 = 34416$  pulse which corresponds to a denser structure. If the intensity falls up to the value  $I = I_3/2 = 17208$  pulse, the value  $2\theta_c = 0.526^\circ$ , and  $\theta_c = 0.263^\circ = 4.590$  mrad. This corresponds to a density  $\rho = 3.25 \text{ g/cm}^3$ , which is close to the density of silicon carbide -  $3.2 \text{ g/cm}^3$ .

The layer thickness is determined by the formula  $2d \sin \theta = \lambda$ , or taking into account the small values of  $\theta$ :  $d = \lambda/2 \theta$  nm, where  $\lambda$  - the wavelength of  $CuK_\alpha$  (0.154 nm) or  $CuK_\beta$  (0.139 nm)

radiation, and  $2\theta_{av}$  was determined as an average from several  $(j - i)$  peaks (Table 3). To determine the thickness, four narrow peak of SiC, and two broad bands of SiO<sub>2</sub>, probably from two different phases - cristobalite and quartz (Fig. 15), were used. The second broad band consists of 3 bands. The thickness of the resulting system (SiO<sub>2</sub> – SiC<sub>0.7</sub> – Si) was about 100 nm.

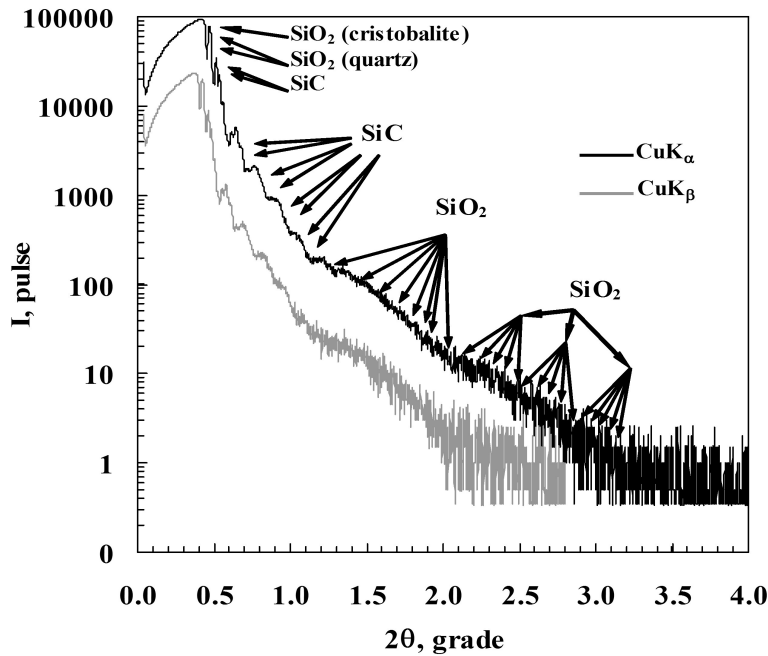


**Figure 15.** X-ray reflectometry using two spectral lines CuK<sub>α</sub> (0.154 nm) and CuK<sub>β</sub> (0.139 nm) ("ComplexXRay C6") of parameters of the SiC<sub>0.7</sub> films, synthesized by multiple implantation of carbon ions with energies of 40, 20, 10, 5 and 3 keV into silicon, after annealing at 1250°C.

Layer	$(2\theta)_j$	$(2\theta)_i$	$j - i$	$2\theta_{av} = [(2\theta)_j - (2\theta)_i] / (j - i)$	$\lambda$	$d = \lambda / 2\theta, \text{ nm}$
SiC	1.138	0.598	4	0.135	0.15405	65.4
SiO <sub>2</sub>	3.154	2.012	3	0.38	0.15405	23.2
SiO <sub>2</sub>	2.012	1.178	1	0.83	0.15405	10.6

**Table 3.** Determination of the thickness of the layers in the system (SiO<sub>3</sub> – SiC<sub>0.7</sub> – Si) by X-ray reflectometry according equation  $2d \cdot \sin \theta = \lambda$ .

Similar measurements for the SiC<sub>0.95</sub> layer also led to the observation of the intensity oscillations of X-ray reflections. The first maximum of reflection with intensity  $I_1 = 98703$  pulses at an angle of  $2\theta = 0.396^\circ$  is observed (Fig. 16). The critical angle of total external reflection is evaluated as an angle where  $I = I_1/2 = 49352$  pulses, but in this case in the position of a minimum  $I = 53961$  pulse, i.e.  $2\theta_c = 0.458^\circ$ , and  $\theta_c = 0.229^\circ = 3.979 \text{ mrad}$ . This angle corresponds to the film density  $2.46 \text{ g/cm}^3$ , which is close to the density of optical glass  $2.51 \text{ g/cm}^3$ . Further, with increasing of incidence angle, the intensity of reflection is again increased up to  $I_2 =$

57255 pulses, which indicates the occurrence of a more dense structure. If the intensity falls up to the value  $I = I_2/2 = 28627$  pulses, the value  $2\theta_c = 0.510^\circ$ , the critical angle is equal to  $\theta_c = 0.255^\circ = 4.451$  mrad. This corresponds to a density  $3.06 \text{ g/cm}^3$ , which is close to the density of silicon carbide -  $3.2 \text{ g/cm}^3$ .

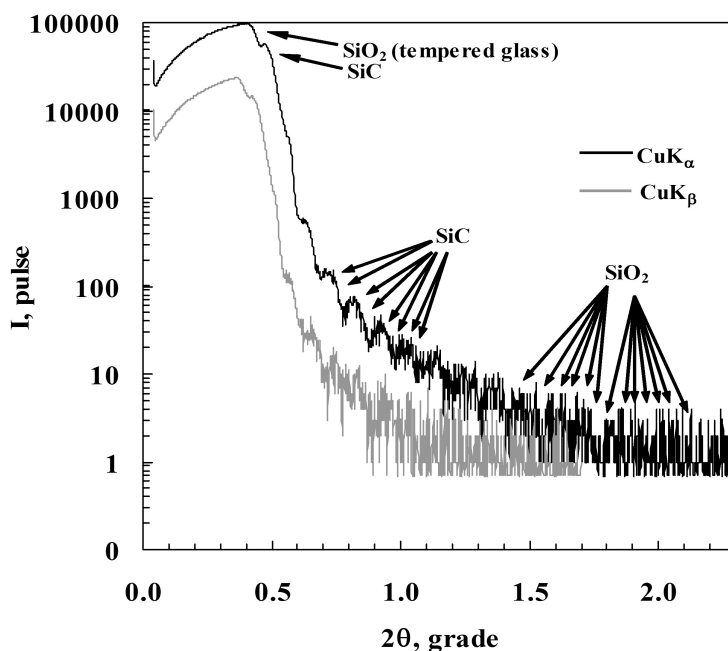


**Figure 16.** X-ray reflectometry of parameters of the films  $\text{SiC}_{0.95}$ , synthesized by multiple implantation of carbon ions with energies of 40, 20, 10, 5 and 3 keV into silicon after annealing at  $1150^\circ\text{C}$ .

To determine the thickness of the layers, four narrow peaks of SiC, and two broad bands of  $\text{SiO}_2$  (Fig. 16) were used.

Layer	$(2\theta)_j$	$(2\theta)_i$	$j - i$	$2\theta_{av} = [(2\theta)_j - (2\theta)_i] / (j - i)$	$\lambda$	$d = \lambda / 2\theta, \text{ nm}$
SiC	1.066	0.690	4	0.094	0.15405	93.9
$\text{SiO}_2$	2.19	1.426	2	0.382	0.15405	23.1

**Table 4.** Determination of the thickness of the layers in the system  $(\text{SiO}_{2.33} - \text{SiC}_{0.95} - \text{Si})$  by X-ray reflectometry.

The thickness of the system  $(\text{SiO}_{2.33} - \text{SiC}_{0.95} - \text{Si})$  was 117 nm, which was comparable to the estimated thickness of the film.  $\text{SiO}_2$  peaks are visible not clearly. Perhaps this is because the annealing temperature was taken at  $100^\circ\text{C}$  lower ( $1150^\circ\text{C}$ ).

### 3.2.2 The study of the high-temperature instability of solid $\text{SiC}_{0.7}$ films synthesized by ion implantation

In Fig. 17, the IR transmission spectra of the homogeneous  $\text{SiC}_{0.7}$  films, synthesized on substrates of Si(100) with resistivity 4–5 Ohm cm (a) and Si(111) with resistivity 10 Ohm cm (b), subjected to isothermal annealing at the temperature 1200°C for several hours in an atmosphere of inert gas (Ar), are presented. Comparing these two figures (a) and (b), one can see that the nature of the SiC films formed on substrates with different crystallographic orientations, are different. This difference manifests itself in the amplitudes and half-widths of the peaks corresponding to the excitation of both transverse and longitudinal optical lattice oscillations of SiC (TO- and LO-phonons).

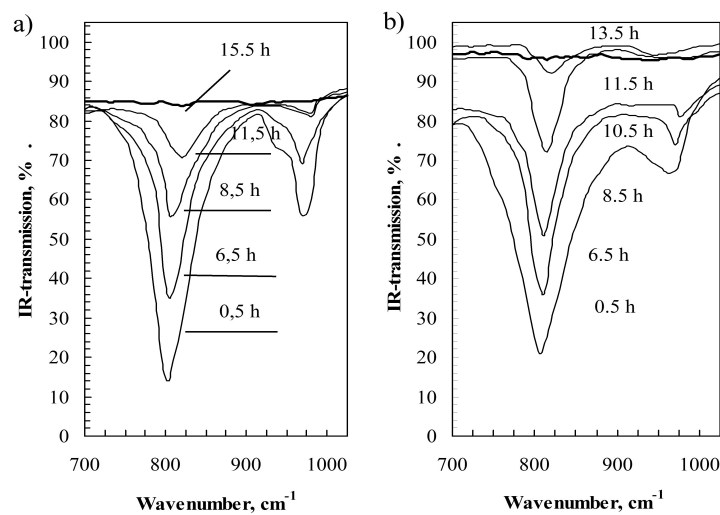


**Figure 17.** The dependence of the IR transmission spectra of implanted by  $^{12}\text{C}^+$  ions Si on the annealing time at the temperature 1200°C: a) n-Si, the orientation of substrate Si(100), b) p-Si, the orientation of substrate Si(111).

After annealing at 1200°C for 30 min in the IR spectra an intense peak at 800  $\text{cm}^{-1}$  which associated with the TO phonons of SiC, as well as a peak at 960  $\text{cm}^{-1}$  corresponding to the LO-phonons of SiC, are observed. It is seen that in contrast to the spectra of film on (100) oriented Si substrate, the transmission spectra of oscillation modes of SiC of film on the (111) oriented silicon substrate are more blurred and the level of the transmission spectra of the two modes are superimposed on each other, and does not achieve the initial zero level in the wave number, equal to 915  $\text{cm}^{-1}$ . This is caused by the half-width of these peaks (Fig. 17 and 18).

The narrowing of the peak (Fig. 18) up to 40  $\text{cm}^{-1}$  occurs as a result of intensive formation of the tetrahedrally oriented Si–C-bonds absorbing at 800  $\text{cm}^{-1}$ , as well as the decay of bonds which absorb at frequencies different from the value of 800  $\text{cm}^{-1}$ . Since the tetrahedral bond corresponds to the crystalline phase of silicon carbide, the narrowing of the peak of the IR spectrum with a minimum at 800  $\text{cm}^{-1}$  is associated with the process of ordering of the implanted layer. As is seen from Fig. 18, for the  $\text{SiC}_{0.7}$  layer the narrowing of the peak is more intense with increasing time of isothermal annealing up to 6.5 hours in the case of the (111) oriented substrate in comparison with (100) orientation. After annealing for 8.5 hours or

more a further narrowing of the peak is slowing, indicating a complete processes of SiC lattice ordering. Thus, it was established that the annealing duration of the less than 6.5 hours at 1200°C is insufficient to form the structure of silicon carbide.

As is seen from Figs. 17 and 19, the amplitude values of the peaks with increasing of annealing time at 1200°C are reduced. This indicates a decrease in the total volume of silicon carbide due to disintegration of SiC and desorption of carbon. Since the amplitude of the SiC-peak of infrared transmission is proportional to the concentration of Si-C-bonds, the measurements of its value were made in the spectra after isothermal annealing at the temperature of 1200°C (Fig. 19). For (100) oriented silicon substrate of n-type conductivity, the amplitude of the TO- and LO-phonon peaks of the infrared transmission (Fig. 19, curves 2 and 4) after annealing for 0.5–6.5 hours were higher than the same for (111) oriented silicon, and then the decay of SiC in this layer becomes more intense. However, as is seen from Figs. 17 and 19, after annealing for 11.5 and 13.5 hours the disintegration of silicon carbide is almost finished for the SiC<sub>0.7</sub> layer on the (111) substrate, while for the (100) orientation is observed after annealing during up to 15.5 hours.

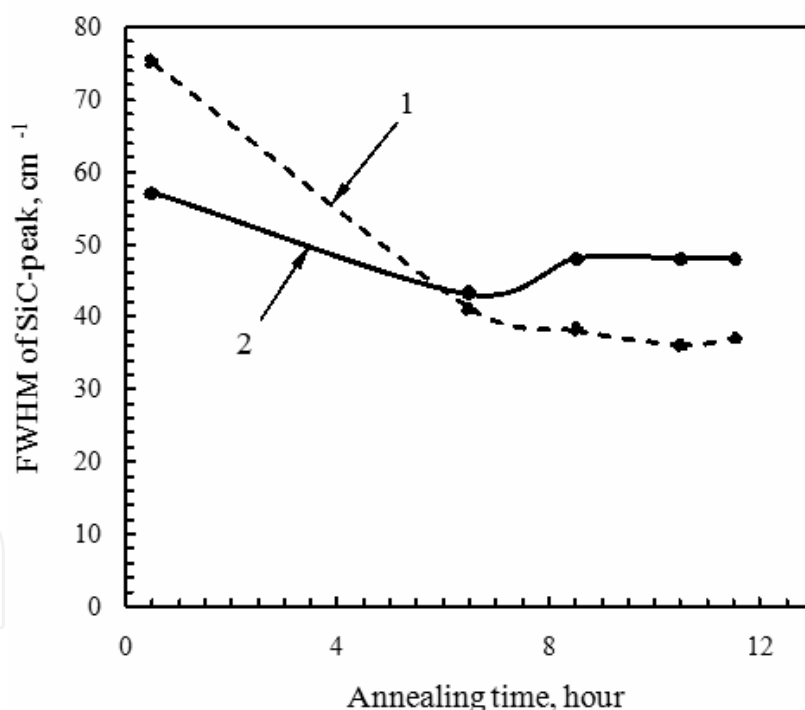


**Figure 18.** Dependence of the half-width of the TO-phonons peak of SiC of IR spectra on the annealing time at the temperature of 1200°C for SiC<sub>0.7</sub> layers: 1 - Si(111) substrate, 2 - Si(100) substrate.

It should be also noted that the signal from the LO-phonons in the spectra of both types of substrate disappears earlier (Fig. 19) than the signal from the TO-phonons, and in particular, at (111) orientation of substrate. Thus, a gradual decrease in the amplitudes of the TO-and LO-phonon peaks of SiC in the IR transmission spectra of ion-synthesized SiC films at the



increasing time of high-temperature annealing indicates the decay of the SiC structure, i.e. the instability of these films to such regime of treatment.

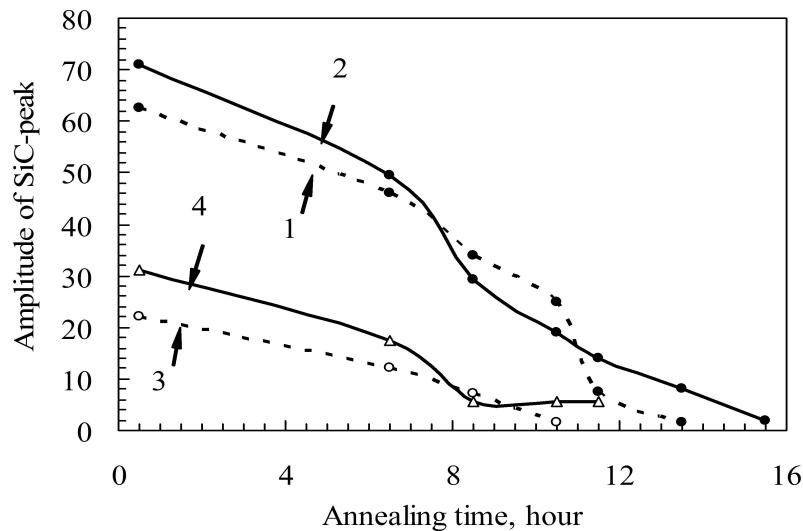


**Figure 19.** Amplitude of TO- and LO-phonon peaks of SiC of IR transmission versus the annealing time at the temperature of 1200°C for SiC<sub>0.7</sub> layers on silicon substrates of (100) and (111) orientation: 1 – Si(111), TO-phonon peak; 2 – Si(100), TO-phonon peak; 3 – Si(111), LO-phonon peak; 4 – Si(100), LO-phonon peak.

Since the amplitude of the infrared transmission at the wavenumber 800 cm<sup>-1</sup> is proportional to the concentration of the tetrahedrally oriented Si–C-bonds, its magnitudes were measured in the spectra after isothermal annealing at the temperature of 1200°C (Fig. 20, curve 3). Assuming that the amplitude at any frequency is proportional to the number of the Si–C-bonds which absorb at this frequency, the amplitudes for the TO-phonons with wavenumbers 700, 750, 850 and 900 cm<sup>-1</sup> (Fig. 20) in the case of incidence of IR radiation to the sample surface at an angle of 73° to the normal were also measured.

It is seen in Fig. 20a, b (curves 3) that after annealing at 1200°C for 0.5 hour of the SiC<sub>0.7</sub> film on the Si (100) substrate, the amplitude at wavenumber 800 cm<sup>-1</sup> is higher than the same for the Si(111) substrate (70 and 58%), indicating a higher content of the tetrahedrally oriented SiC-bonds. It is also seen that the number of SiC-bonds which are close to tetrahedral orientation and absorb at 750 and 850 cm<sup>-1</sup>, in the case of the substrate Si (100) is lower after annealing for 0.5 h (Fig. 20, curves 2 and 4) in comparison with the substrate Si(111) due to their more intense transformation into the tetrahedral SiC-bonds. The nonlinear nature of the curve 3 in the region 0.5 – 8.5 hours may be due to the formation of tetrahedrally oriented SiC-bonds in the layer simultaneously with their decay at the surface. The saturation of this process after annealing during 6.5 hours results in a faster decrease in the number of bonds during further annealing.

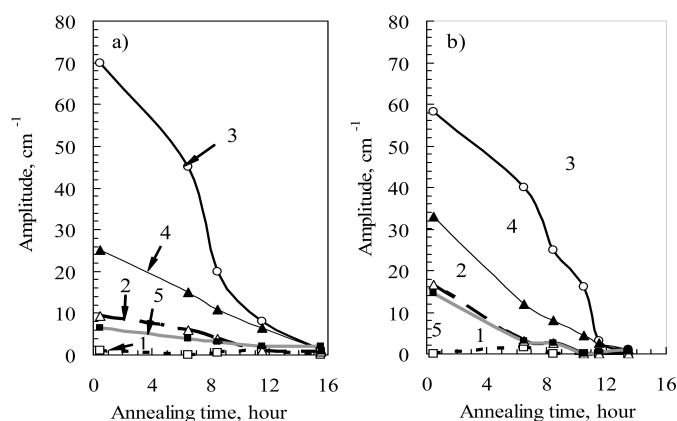


**Figure 20.** The amplitude of the infrared transmittance at fixed wavenumbers versus the duration of isothermal annealing of the  $\text{SiC}_{0.7}$  layer (angle of incidence of infrared rays on the sample is  $73^\circ$  from the normal): 1 –  $700\text{ cm}^{-1}$ , 2 –  $750\text{ cm}^{-1}$ , 3 –  $800\text{ cm}^{-1}$ , 4 –  $850\text{ cm}^{-1}$ , 5 –  $900\text{ cm}^{-1}$ ; a) the substrate orientation Si (100), b) the substrate orientation Si (111).

This process is clearly demonstrated on the time dependence of the area of SiC-peak, which is proportional to the total number of optically active Si–C-bonds (Fig. 21). Although the peak amplitude at the minimum of IR transmission (Fig.19, curve 2) and at  $800\text{ cm}^{-1}$  (Fig.20, curve 3) for the Si substrates with (100) orientation are higher than in the case of (111) orientation, the value of area of SiC-peak for (111) was higher after annealing for 0.5 hours. This is due to a greater half-

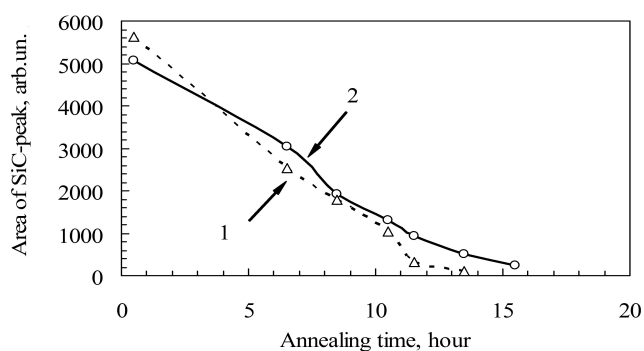


**Figure 21.** The area of the TO-phonon peak of SiC in spectra of the IR transmission versus the annealing time at the temperature of  $1200^\circ\text{C}$  for the  $\text{SiC}_{0.7}$  layers (angle of incidence of infrared rays on the sample surface -  $73^\circ$  from the normal): 1 - the orientation of the substrate Si(111), 2 – the orientation of the substrate Si(100).

width of the peak caused by a significant amount of optically active Si–C-bonds close to tetrahedrally oriented, which absorb at  $750$  and  $850\text{ cm}^{-1}$  and, probably due to the smaller amount of stable carbon silicon clusters in the film on (111) oriented silicon substrate. It is not contradict to the data for the SiC layer with Gaussian distribution of carbon in silicon, for which was shown that immediately after the implantation of carbon into the (100) and (111) oriented silicon at least 65% and 60% of carbon atoms are concentrated in optically inactive clusters, respectively (see 3.1.2, Fig. 6 “The temperature range  $20\text{-}600^\circ\text{C}$ ”). The strong carbon

clusters prevent the crystallization of SiC, and they are less susceptible to oxidation and prevent the penetration of oxygen into the SiC-layer. The SiC film on (100) substrate has more quantity of stable clusters after implantation and, as a result the smaller value of area of SiC-peak and smaller amount of optically active Si-C-bonds after annealing for 0.5 hours and, it less susceptible to oxidation at 1200°C – 15.5 h (instead of 13.5 h for (111) Si substrate). The relatively rapid decay of close to tetrahedral Si-C bonds (Fig. 20b, curves 2 and 4) led to the decrease with higher speed of the number of optically active Si-C-bonds in the case of (111) orientation of Si substrate. In general the dependence of the reduction of optically active Si-C-bonds on the annealing time is linear. This implies that the rapid decay of close to tetrahedral Si-C-bonds was occurring, mainly, due to their transformation into a tetrahedral bond. The linear dependence indicates the homogeneity of the layer, and a rectangular profile of the distribution of carbon atoms in silicon, as well as the fact that the decay rate of silicon carbide does not depend on the depth of the oxidation front. Some decrease in the slope of angle of the curves at the end of the annealing is occurring due to oxidation of the interface "the SiC film – Si substrate".

The value of the wave number of the minimum of SiC-peak of the infrared transmission (the position of the minimum of peak) defines a prevailing kind of optically active bonds which absorb at this wavenumber at this temperature. For the considered layers after annealing at 1200°C for 0.5 h, the transmission peaks with values of minimum at wavenumbers 803 and 806  $\text{cm}^{-1}$ , characteristic of crystalline silicon carbide, are observed (Fig. 22). It was found that with increasing annealing time, the position of the peak minimum varies smoothly and moved in the direction of the wave number increase (Fig. 17 and 22).

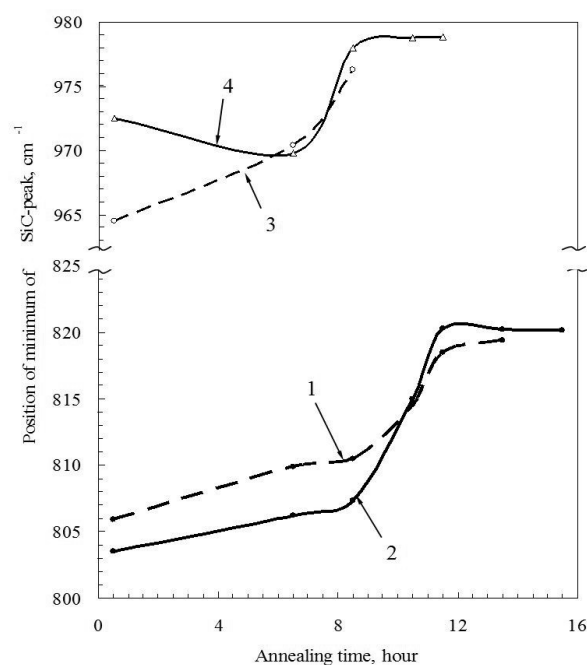


**Figure 22.** Wave number of the minimum of SiC-peak of IR transmission versus the annealing time at 1200°C for the  $\text{SiC}_{0.7}$  layers on silicon substrates of (100) and (111) orientations: 1 - Si (111), TO-phonons, 2 - Si(100), TO-phonons, 3 - Si(111), LO-phonons, 4 - Si(100), the LO-phonons.

In our opinion, the frequency shifts of SiC-peak upward indicate a decrease in crystallite size of SiC. We have previously identified size effects, which manifested in the influence of the crystallite sizes of silicon carbide on its optical properties. It was shown (Fig.23) that the differences of the  $\text{SiC}_{0.03}$ ,  $\text{SiC}_{0.12}$  and  $\text{SiC}_{0.4}$  layers with low carbon concentration from the  $\text{SiC}_{1.4}$ ,  $\text{SiC}_{0.95}$  and  $\text{SiC}_{0.7}$  layers with high carbon concentration are manifested in the absence of LO-phonon peak of SiC in the IR transmission spectra and in a shift at  $1000^\circ\text{C}$  of minimum SiC-peak for TO-phonons in the region of wave numbers higher than  $800\text{ cm}^{-1}$ , characteristic for the tetrahedral bonds of crystalline SiC, which is caused by small sizes of SiC crystallites ( $\leq 3\text{ nm}$ ) and by an increase of contribution in the IR absorption of their surfaces, and the surfaces of Si crystallites containing strong short Si-C-bonds as well.

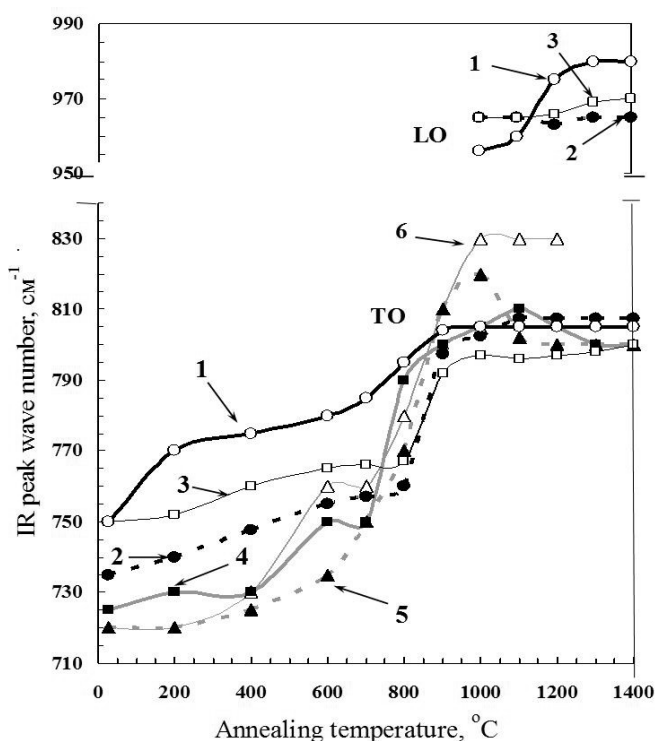


**Figure 23.** Wavenumber of the IR transmission peak for TO- and LO-phonons SiC as a function of the annealing temperature: 1 -  $\text{SiC}_{1.4}$ , 2 -  $\text{SiC}_{0.95}$ , 3 -  $\text{SiC}_{0.7}$ , 4 -  $\text{SiC}_{0.4}$ , 5 -  $\text{SiC}_{0.12}$ , 6 -  $\text{SiC}_{0.03}$ .

In this case (Fig. 22), the increase of annealing duration of  $\text{SiC}_{0.7}$  layer leads to both the shift of the minimum of the IR transmission peak up to  $820\text{ cm}^{-1}$ , and the reduction of the amplitude of the LO-phonon peaks and their subsequent disappearance, although  $\text{SiC}_{0.7}$  is considered as the layer with a high concentration of carbon. At the same time more intense process of the shift of the minimum of SiC-peak occurs after annealing for longer than 8.5 hours, which leads to the disappearance of the peak of LO-phonons. This can occur when the penetration of oxygen deep into the layers, their interaction with the carbon atoms on the surface of the crystallites of silicon carbide with the formation of molecules of  $\text{CO}/\text{CO}_2$ . Desorption of carbon atoms causes a decrease in the size of the SiC crystallites and their disintegration. With increasing duration of annealing, the homogeneous  $\text{SiC}_{0.7}$  layer entirely transforms into

SiO<sub>2</sub>, and then goes the oxidation of the interface “SiC film – Si substrate”, in which the carbon concentration decreases uniformly with depth according to a Gaussian law. Thus, the concentration of carbon in the remaining layer begins to decrease. This leads to the appearance of phenomenon which is characteristic for the SiC<sub>0.4</sub>, SiC<sub>0.12</sub>, SiC<sub>0.03</sub> layers, namely, to shift of the minimum of the IR transmission peak up to 820 cm<sup>-1</sup>, and to a decrease of the amplitude of the LO-phonon peak and their subsequent disappearance. Thus, size effects are confirmed, published by us in 2011.

### 3.3. Parameters of SiC and C films on Si substrates synthesized by magnetron and ion-beam sputtering

#### 3.3.1. Parameters of C films on Si substrates synthesized by by magnetron sputtering

Carbon thin films were obtained by reactive magnetron sputtering using an ARC 2000 system. A graphite target with a diameter ~50 mm and a thickness of 3 mm was used. The magnetron sputtering mode parameters were: cathode voltage  $U_c = 470$  V, the ion beam current  $I_{ion} = 35$  mA and the argon pressure inside the chamber ~1 Pa. The carbon films were deposited on a set of cleaned silicon substrates. The temperature of the substrate was 75°C.

The presence of a sharp interface "C film - Si substrate" permits to investigate the thickness and density of the film by X-ray reflectometry (CompleXRy C6) by recording the angular dependence of the reflection coefficient using two spectral lines CuK<sub>α</sub> (0.154 nm) and CuK<sub>β</sub> (0.139 nm). The oscillations of intensity were observed, assigned to the interference of X-ray reflections from the boundaries of carbon layer (Fig. 24).

It is known that the density of graphite is 2.2 g/cm<sup>3</sup> and the density of diamond - 3.51 g/cm<sup>3</sup>. Since the density of the resulting film was 3.32 g/cm<sup>3</sup> (Table 5 and Fig.24), we concluded that the diamond-like carbon film was synthesized.

Layer	$I_{max}$	$I_{max}/2$	$2\theta_c$	$\theta_c$ , grade	$\theta_c$ , rad	$\rho$ , g/cm <sup>3</sup>
C	962849	481425	0.529	0.2645	4.616	3.32

**Table 5.** Determination of the density of the carbon layer by X-ray reflectometry and using the Henke program.

To determine the thickness, five narrow peaks of C, and a broad band of C were used (Fig. 24, table 5).

Layer	$(2\theta)_j$	$(2\theta)_i$	$j - i$	$2\theta_{av} = [(2\theta)_j - (2\theta)_i] / (j - i)$	$\lambda$ , nm	$d = \lambda / 2\theta$ , nm
C	1.684	1.164	5	0.104	0.15405	84.9
C	2.732	2.080	1	0.652	0.15405	13.5

**Table 6.** Determination of the thickness of the layers in the system (C - C - Si) by X-ray reflectometry.



Simulation using the Henke program ([http://henke.lbl.gov/optical\\_constants/](http://henke.lbl.gov/optical_constants/)) [24] allows to obtain a theoretical curve, which is close to the experimental (Fig.25). The main parameters of the layer system, which allow to obtain an acceptable agreement of experimental and theoretical curves, were:

1. the diamond-like carbon film of thickness  $d = 84$  nm, density  $\rho = 3.3$  g/cm<sup>3</sup>, and surface roughness  $\sigma = 1.5$  nm;
2. a thin graphite layer of thickness  $d = 5$  nm with the density  $\rho = 2.206$  g/cm<sup>3</sup>, and the roughness of (C- C) interface  $\sigma = 0.13$  nm;
3. the silicon substrate with density  $\rho = 2.33$  g/cm<sup>3</sup> and the roughness of interface (C-Si)  $\sigma = 0$  nm.

Thus, diamond-like carbon film of thickness  $d = 84$  nm, density  $\rho = 3.3$  g/cm<sup>3</sup>, and surface roughness of  $\sigma = 1.5$  nm on a silicon surface by magnetron sputtering was synthesized.

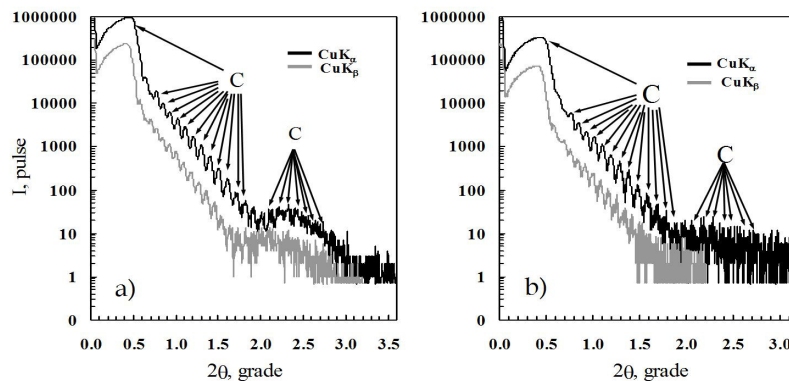


**Figure 24.** X-ray reflectometry using two spectral lines  $\text{CuK}_\alpha$  (0.154 nm) and  $\text{CuK}_\beta$  (0.139 nm) (CompleXRy C6) of parameters of carbon films synthesized by magnetron sputtering: a) sample A; b) sample B.

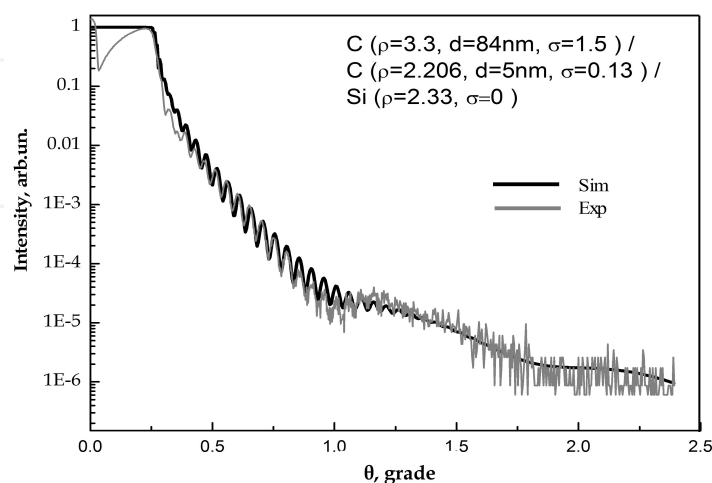


**Figure 25.** Simulation using the Henke program [24] of experimental results obtained by X-ray reflectometry of parameters of carbon films synthesized by magnetron sputtering.

### 3.3.2. Parameters of SiC films on Si substrates synthesized by ion-beam sputtering

SiC films were prepared by ion-beam sputtering. For the simultaneous deposition on silicon substrates of C and Si atoms, a two-component target consisting of the overlapping wafers of silicon and graphite was used. Sputtering of the target was carried out in an argon atmosphere. The formation of Ar ion beam was happening in the ring electrode system (a hollow cathode and an anode), and magnets with crossed electrical and magnetic fields. Discharge power was 108 W (2.7 kV, 40 mA), argon pressure in the chamber  $5.9 \times 10^{-2}$  Pa, substrate temperature - 20°C. Samples with SiC films were annealed at 1250°C in an argon atmosphere for 30 min.

The presence of a sharp interface "the SiC film - Si substrate" permits to investigate the thickness and density of the film by X-ray reflectometry ("ComplexXRay C6"). The oscillations of intensity were observed, assigned to the interference of X-ray reflections from the boundaries of silicon carbide layer (Fig. 26). It is known that the density of graphite is 2.2 g/cm<sup>3</sup>, and of silicon - 2.33 g/cm<sup>3</sup>, of silicon carbide - 3.2 g/cm<sup>3</sup> and of diamond - 3.51 g/cm<sup>3</sup>. Since the density of the obtained film was 3.03 g/cm<sup>3</sup> (Table 6 and Fig.26), we concluded, that the film close to silicon carbide, was synthesized. The film contains approximately  $[(3.03-2.33)/(3.2-2.33)] \times 100\% = 80.5\%$  SiC, and  $[(3.2-3.03)/(3.2-2.33)] \times 100\% = 19.5\%$  Si, i.e., about 80 atoms of C refer per 100 atoms of Si and the SiC<sub>0.8</sub> layer was formed.

Layer	$I_{\max}$	$I_{\max}/2$	$2\theta_c$	$\theta_c$ , grade	$\theta_c$ , rad	$\rho$ , g/cm <sup>3</sup>
SiC	101255	50628	0.508	0.254	4.433	3.03

**Table 7.** Determination of the density of the SiC layer by X-ray reflectometry and using the Henke program.

To determine the film thickness the position of maxima of five narrow peaks of SiC was used (Fig.26).

Layer	$(2\theta)_j$	$(2\theta)_i$	$j-i$	$2\theta_{av} = [(2\theta)_j - (2\theta)_i] / (j-i)$	$\lambda$ , nm	$d = \lambda / 2\theta$ , nm
SiC	1.230	1.034	4	0.0490	0.15405	180.1

**Table 8.** Determination of the thickness of the layer in the system (SiC - Si) by X-ray reflectometry.

Simulation using the Henke program ([http://henke.lbl.gov/optical\\_constants/](http://henke.lbl.gov/optical_constants/)) [24] allows obtaining a theoretical curve, which is close to the experimental (Fig.27). The main parameters of the layer system, which allow to obtain an acceptable agreement of experimental and theoretical curves, were:

1. the silicon carbide film of thickness  $d = 160$  nm, the density  $\rho = 3.03$  g/cm<sup>3</sup>, and surface roughness of  $\sigma = 0.4$  nm;
2. the silicon substrate with density  $\rho = 2.33$  g/cm<sup>3</sup> and the roughness of interface (SiC-Si)  $\sigma = 1.5$  nm.

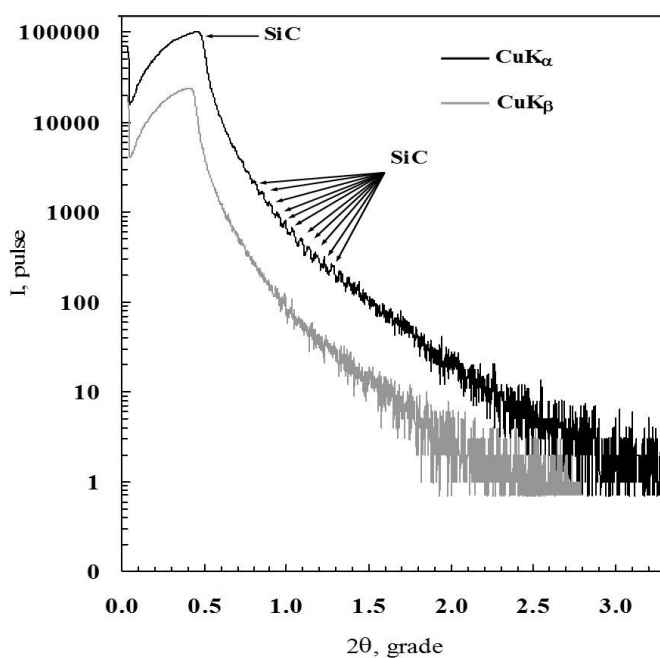


**Figure 26.** X-ray reflectometry using two spectral lines  $\text{CuK}_\alpha$  (0.154 nm) and  $\text{CuK}_\beta$  (0.139 nm) (CompleXRy C6) parameters of silicon carbide films synthesized by ion-beam sputtering of the two-component target of silicon and graphite.

The film thickness  $d = 160$  nm is different from the values of 180 nm, obtained from the average distance between the peaks  $2\theta_{\text{av}}$ . The reasons for the differences require further studies.

Thus, the silicon carbide film of thickness  $d = 160$  nm, the density  $\rho = 3.03$  g/cm<sup>3</sup>, and surface roughness of  $\sigma = 0.4$  nm on the silicon surface by ion-beam sputtering of the two-component target of silicon and graphite was synthesized.

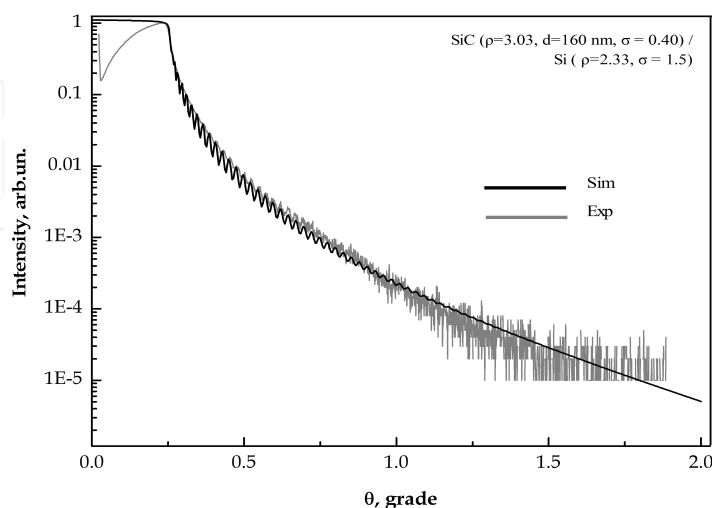


**Figure 27.** Simulation using the Henke program [24] of experimental results obtained by X-ray reflectometry of parameters of SiC films synthesized by ion-beam sputtering of the two-component target of silicon and graphite.

### Conclusion

1. For silicon layer with the Gaussian profile of implanted carbon atoms, the peak of longitudinal optical oscillations (LO-phonons) of SiC at  $965\text{--}970\text{ cm}^{-1}$  is found and, it permits to calculate a number of optical parameters of film. The values of the low-frequency dielectric constant,  $\epsilon_0$ , the effective charge,  $e^*/e$ , and the dimensionless parameter,  $\rho$ , are equal to 9.82, 0.89, and 0.25, respectively. The dependences of LO-phonon peak amplitude, halfwidth and peak position from both an angle of incidence of the electromagnetic radiation on sample surface and the annealing temperature are determined. The difference between the LO-phonon curves behaviour indicates that the formation of SiC crystallites, i.e. the intensive formation of tetrahedral Si–C-bonds of necessary length and bond angles, in the case of (111) oriented substrate is not completed up to the silicon melting point, as for (100) oriented substrate that is completed at  $1350^\circ\text{C}$ .
2. The temperature dependence of an area under contour of IR spectrum curve in wide temperature range  $200\text{--}1400^\circ\text{C}$  was used to obtain valuable new information about the structure transformation in the carbon implanted silicon layer. The high sensitivity of temperature dependence of area to a change of substrate orientation was found.
3. A model of the ion implanted layer in the form of the system of the carbon-silicon clusters consisting of the carbon- and silicon atoms linked one with another by single-, double- and tripple bonds, and by single elongated-, sesqui, free ("dangling") and hybridized bonds, as well as resonances, is discussed. The infrared inactive flat nets and chains tied together by the infrared active clusters and, by tetrahedrally oriented bonds which are characteristic for silicon and silicon carbide, are described. Immediately after the implantation of carbon into the (100) and (111) oriented silicon at least 65% and 60% of carbon atoms are concentrated in these optically inactive clusters, respectively, if the implantation was carried out by a dose to obtain the stoichiometric concentration ( $E = 40\text{ keV}$ ,  $D = 3.56 \times 10^{17}\text{ cm}^{-2}$ ) of carbon and silicon. An over-barrier mechanism of the formation of Si and SiC crystallites is supposed and it explained by tendency of an isolated system to a minimum of free energy.
4. For carbon implanted silicon layer ( $E = 40\text{ keV}$ ,  $D = 3.56 \times 10^{17}\text{ cm}^{-2}$ ) on (100) and (111) substrate the crystallization process in several temperature ranges was studied. For (100) oriented Si substrate it was shown:
  - $20\text{--}600^\circ\text{C}$  – the formation of tetrahedrally oriented Si–C-bonds due to disintegration of clusters which consist mainly of the Si–Si, Si=Si and elongated Si–C-bonds;
  - $600\text{--}800^\circ\text{C}$  – the formation of Si crystallites and tetrahedrally oriented Si–C-bonds due to disintegration of strained Si–Si bonds and Si–C-bonds, which absorb at frequencies close to  $700$  and  $750\text{ cm}^{-1}$ , recrystallization starts near the substrate and the surface and goes to the middle of layer;
  - $800\text{--}1000^\circ\text{C}$  – begins to dominate the absorption at  $800\text{ cm}^{-1}$ , and near it, due to formation of tetrahedrally oriented bonds of the SiC crystallites, as well as bonds close to tetrahedral;
  - $1000\text{--}1100^\circ\text{C}$  - the growth of the crystallite size through consolidation of small crystallites of Si and SiC; decay of Si–C-bonds absorbing at  $850$  and  $900\text{ cm}^{-1}$ ;

- 1100–1200°C – formation of new optically active clusters absorbing at frequencies of 750, 850 and 900  $\text{cm}^{-1}$  due to the decay of optically inactive clusters;
  - 1200–1250°C – the transformation of clusters absorbing at frequencies of 800–900  $\text{cm}^{-1}$ , into clusters, which absorb at 700 and 800  $\text{cm}^{-1}$ , and the growth of SiC crystallite size;
  - 1250–1300°C – intensive decay of the tetrahedral Si–C-bonds, caused by the desorption of carbon and the destruction of small crystallites;
  - 1300–1350°C – the decay of stable clusters with multiple bonds and the increase in the number and size of crystallites of SiC, and Si–C-bonds, close to tetrahedral;
  - 1350–1400°C – a significant decrease of amount of the polycrystalline SiC due to desorption of carbon atoms.
5. An influence of substrate orientation on  $\beta$ -SiC formation has been studied. It was shown that the SiC-synthesis in the temperature range 900–1000°C is more preferable on (100) oriented silicon substrates and at 1200–1300°C – on (111) oriented silicon substrates. In the case of the (100) oriented substrate the number of tetrahedrally oriented Si–C-bonds reached at 1000°C some maximum and does not change up to 1200°C, whereas in the case of orientation (111) the number of bonds increases smoothly in the range 900–1300°C.
  6. Using thermo-emf, it was determined a type of conduction of Si- and SiC-crystallites. The SiC-crystallites have p-type of conduction independently from the type of conduction of substrate, while the Si-crystallites have the same conduction as a substrate.
  7. During the prolonged high-temperature isothermal annealing (1200°C) a gradual decrease in the amplitude of the TO- and LO-phonon peaks of IR transmission, characteristic of ion-synthesized SiC, indicates the disintegration of the structure of homogeneous SiC film, ie the instability of these films at these temperatures.
  8. It is shown that the deformation of the rectangular Auger profile of  $\text{C}^{12}$  distribution in Si in comparison with the calculated profile, namely the thinning of the interface "the SiC film – Si substrate", and the increase of the carbon concentration at the surface and in regions near the maxima of the distributions for individual carbon ion energy (40, 20 keV), is caused by both the surface sputtering and the change in the composition of the silicon layer during high dose implantation of carbon.
  9. The presence of a sharp interface "the SiC film – Si substrate" permits to study the composition, the density and the thickness of the  $\text{SiC}_{0.7}$  and  $\text{SiC}_{0.95}$  films by X-ray reflectometry (CompleXRay C6) at small grazing angles  $\theta$  by recording the angular dependence of the reflection coefficient using two spectral lines  $\text{CuK}_\alpha$  (0.154 nm) and  $\text{CuK}_\beta$  (0.139 nm), although this method for ion-implanted layers usually does not apply. Using the Henke program for  $\text{SiC}_{0.7}$  film was determined a surface layer with density 2.37  $\text{g/cm}^3$ , which is close to cristobalite ( $\text{SiO}_2$ ) 2.32  $\text{g/cm}^3$ . Further located the film with a density 2.77  $\text{g/cm}^3$  and is close to quartz ( $\text{SiO}_2$ ) 2.65  $\text{g/cm}^3$ . A structure of thickness 65 nm and density  $\rho = 3.25 \text{ g/cm}^3$ , is close to the silicon carbide - 3.2  $\text{g/cm}^3$ . The study of  $\text{SiC}_{0.95}$  film show the presence of surface layer with density 2.51  $\text{g/cm}^3$  (optical glass) and the silicon carbide layer of thickness 94 nm and density 3.06  $\text{g/cm}^3$ .



10. It is shown that the decomposition of optically active Si–C-bonds is more intense in the case of the (111) orientation of the silicon substrate. Based on the linear nature of reducing the number of Si–C-bonds in a homogeneous SiC<sub>0.7</sub> layer with increasing annealing time, it was concluded that the decay rate of silicon carbide does not depend on the depth of the oxidation front.
11. It was confirmed the size effect caused by the small size of nanocrystals, which are manifested in the shift of the minimum of the peak of IR transmission up to to 820 cm<sup>-1</sup>, the decrease of the amplitude of the LO-phonon peak and its subsequent disappearance during the oxidation of the interface “SiC film - Si substrate”, where the concentration of carbon atoms decreases.
12. Diamond-like carbon film of thickness  $d = 84$  nm, density  $\rho = 3.3$  g/cm<sup>3</sup>, and surface roughness of  $\sigma = 1.5$  nm on a silicon surface by magnetron sputtering was synthesized. The silicon carbide film of thickness  $d = 160$  nm, the density  $\rho = 3.03$  g/cm<sup>3</sup>, and surface roughness of  $\sigma = 0.4$  nm on the silicon surface by ion-beam sputtering of the two-component target of silicon and graphite was synthesized. Simulation using the Henke program allows obtain theoretical curves, which are close to the experimental curves.

## Author details

Kair Kh. Nussupov\* and Nurzhan B. Beisenkhanov

\*Address all correspondence to: rich-famouskair@mail.ru

Kazakh-British Technical University, Kazakhstan

## References

- [1] Afanas'ev, A. V., Il'in, V. A., Korlyakov, A. V., Lebedev, A. O., Luchinin, V. V., & Tairov, Yu. M. (2011). Karbid kremniya. Vklad SPbGETU « LETI». Priznanie i perspektivy. V kn.: Fizika i tekhnologiya mikro- i nanosistem. S. 50-86. (Silicon carbide. The contribution of SPbGETU "LETI". Recognition and prospects. *In the book. Physics and technology of micro-and nanosystems. P.50-86*). Edited by Luchinin V.V. and Malinovski V.V. Publisher "Russian Collection". St. Petersburg, 239, in Russian.
- [2] Akimchenko, I. P., Kisseleva, K. V., Krasnopevtsev, V. V., Milyutin, Yu. V., Touryanski, A. G., & Vavilov, V. S. (1977a). The structure of silicon carbide synthesized in diamond and silicon by ion implantation. *Radiation Effects*, 33, 75-80.
- [3] Akimchenko, I. P., Kazdaev, Kh.R, & Krasopevtsev, V. V. (1977b). IK-pogloshenie  $\beta$ -SiC, sintezirovannogo pri ionnoi implantacii C v Si. (IR absorption of  $\beta$ -SiC, synthesized by ion implantation of C into Si). *Fizika i Tekhnika Poluprovodnikov*, T.11, vyp. 10, 1964-1966, in Russian.

- [4] Akimchenko, I. P., Kazdaev, H. R., Kamenskikh, I. A., & Krasnopevtsev, V. V. (1979). Opticheskie i fotoelektricheskie svoistva struktury SiC-Si, poluchennoi pri implantacii ionov ugleroda v kremnii. (Optical and photoelectric properties of the SiC-Si structure, obtained by implantation of carbon ions into silicon). *Fizika i Tekhnika Poluprovodnikov*, T.13, vyp.2, 375-378, in Russian.
- [5] Akimchenko, I. P., Kisseleva, K. V., Krasnopevtsev, V. V., Touryanski, A. G., & Vavilov, V. S. (1980). Structure and optical properties of silicon implanted by high doses of 70 and 310 keV carbon ions. *Radiation Effects*, 48, 7-12.
- [6] Aleksandrov, P. A., Baranova, E. K., Demakov, K. D., Komarov, F. F., Novikov, A. P., & Shiryaev, S. Y. (1986). Sintez monokristallicheskogo karbida kremniya s pomoshyu odnoshagovoi tehniki vysokointensivnogo ionnogo legirovaniya. (Synthesis of single-crystal silicon carbide by using one-step technique of high-intensity ion implantation). *Fizika i Tekhnika Poluprovodnikov*, T.20, 1, 149-152, in Russian.
- [7] Aleksandrov, P. A., Baranova, E. K., Gorodetski, A. E., Demakov, K. D., Kutukova, O. G., & Shemardov, S. G. (1988). Issledovanie raspredeleniya amorfnoi i kristallicheskoi fazy ionno-sintezirovannogo SiC v Si. (The investigation of the distribution of the amorphous and crystalline phases of ion-synthesized SiC in Si). *Fizika i Tekhnika Poluprovodnikov*, T.22, 4, 131-132, in Russian.
- [8] Baranova, E. K., Demakov, K. D., Starinin, K. B., Strelcov, L. N., & Haibullin, I. B. (1971). Issledovanie monokristallicheskih plenok SiC, poluchennykh pri bombardirovke ionami C<sup>+</sup> monokristallov Si. (The study of single-crystal films of SiC, obtained by bombardment by C<sup>+</sup> ions of Si single crystals). *Doklady AN SSSR*, 200, 869-870, in Russian.
- [9] Bayazitov, R. M., Haibullin, I. B., Batalov, R. I., Nurutdinov, R. M., Antonova, L. Kh, Aksenov, V. P., & Mikhailova, G. N. (2003). Structure and photoluminescent properties of SiC layers on Si, synthesized by pulsed ion-beam treatment. *Nucl. Instrum. and Meth. in Phys. Res., B*, 206, 984-988.
- [10] Belov, A. I., Mihailov, A. N., Nikolichev, D. E., Boryakov, A. V., Sidorin, A. P., Grachev, A. P., Ershov, A. V., & Tetelbaum, D. I. (2010). Formation and "white" photoluminescence of nanoclusters in SiO<sub>x</sub> films implanted with carbon ions. *Semiconductors.*, 44(11), 1450-1456.
- [11] Borders, J. A., Picraux, S. T., & Beezhold, W. (1971). Formation of SiC in silicon by ion implantation. *Appl Phys. Lett*, 18(11), 509-511.
- [12] Chen, D., Wong, S. P., Yang, Sh., & Mo, D. (2003). Composition, structure and optical properties of SiC buried layer formed by high dose carbon implantation into Si using metal vapor vacuum arc ion source. *Thin Solid Films*, 426, 1-7.
- [13] Durupt, P., Canut, B., Gauthier, J. P., Roger, J. A., & Pivot, J. (1980). RBS, Infrared and diffraction compared analysis of SiC Synthesis in C implanted silicon. *Mater. Res. Bull.*, 15, 1557-1565.

- [14] Edelman, F. L., Kuznetsov, O. N., Lezheiko, L. V., & Lubopytova, E. V. (1976). Formation of SiC and Si<sub>3</sub>N<sub>4</sub> in silicon by ion implantation. *Radiation Effects*, 29, 13-15.
- [15] Fissel, A., Kaizer, U., Pfennighaus, K., Schroter, B., & Richter, W. (1996). Growth of 6H-SiC on 6H-SiC(0001) by migration enhanced epitaxy controlled to an atomic level using surface superstructures. *Applied Physics Letters*, 68, 1204-1206.
- [16] Fissel, A., Schroter, B., Kaiser, U., & Richter, W. (2000). Advances in the molecular-beam epitaxial growth of artificially layered heteropolytypic structures of SiC. *Appl. Phys. Lett*, 77, 2418-2420.
- [17] Frangis, N., Nejim, F., Hemment, P. L. F., Stoemenos, J., & Van Landuyt, J. (1996). Ion beam synthesis of  $\beta$ -SiC at 950°C and structural characterization. *Nuclear Instruments and Methods in Phys. Res. B*, 112, 325-329.
- [18] Frangis, N., Stoemenos, J., Van Landuyt, J., Nejim, F., & Hemment, P. L. F. (1997). The formation of 3C-SiC in crystalline Si by carbon implantation at 950°C and annealing- a structural study. *Journal of Crystal Growth*, 181, 218-228.
- [19] George, V. C., Das, A., Roy, M., Dua, A. K., Raj, P., & Zahn, D. R. T. (2002). Bias enhanced deposition of highly oriented  $\beta$ -SiC thin films using low pressure hot filament chemical vapour deposition technique. *Thin Solid Films*, 419, 114-117.
- [20] Gerasimenko, N. N., Kuznetsov, O. N., Lezheyko, L. V., Lyubopytova, E. V., Smirnov, L. S., & Edelman, F. L. (1974). Nekotorye svoistva plenok SiC, poluchennykh ionnym vnedreniem v strukture Al-SiC-Si. (Some properties of the SiC films, obtained by ion implantation in the structure of Al-SiC-Si.). *Mikroelektronika*, T.3., Vyp.5, 467-468, in Russian.
- [21] Gibbons, J. F., Johnson, W. S., & Hyloic, S. W. (1975). Projected Range Statistics. *Part 1. 93p. 2nd ed. Dowden, Stroudsburg. PA.*
- [22] Glinka, N.L. (1985). Obshaya khimiya (General chemistry). 24-e izd. Pod red. Rabino-vich V.A. L: *Khimiya.*, 702, in Russian.
- [23] Gupta, S. K., & Akhtar, J. (2011). Thermal Oxidation of Silicon Carbide (SiC)- Experimentally Observed Facts. In the book "Silicon Carbide- Materials, Processing and Applications in Electronic Devices", edited by Moumita Mukherjee, *InTech*, Chapter 9., 207-230.
- [24] Henke, B. L., Gullikson, E. M., & Davis, J. C. (1993). X-ray interactions: photoabsorption, scattering, transmission, and reflection at E=50-30000 eV, Z=1-92. *Atomic Data and Nuclear Data Tables*. [2], 181-342.
- [25] Kerdiles, S., Rizk, R., Goubilleau, F., Perez-Rodriguez, A., Garrido, B., Gonzalez-Varona, O., & Morante, J. R. (2000). Low temperature direct growth of nanocrystalline silicon carbide films. *Mater.Sci.Eng., B*, 69, 530-535.
- [26] Kimura, T., Kagiya, Sh., & Yugo, Sh. (1981). Structure and annealing properties of silicon carbide thin layers formed by ion implantation of carbon ions in silicon. *Thin Solid Films*, 319-327.

- [27] Kimura, T., Kagiya, Sh., & Yugo, Sh. (1982). Characteristics of the synthesis of  $\beta$ -SiC by the implantation of carbon ions into silicon. *Thin Solid Films*, 94, 191-198.
- [28] Kimura, T., Yugo, Sh., Bao, Zh. S., & Adachi, Y. (1989). Formation of silicon carbide layers by the ion beam technique and their electrical properties. *Nuclear Instruments and Methods in Phys. Res., B.*, 39, 238-241.
- [29] Khokhlov, A. F., Pavlov, D. A., Mashin, A. I., & Khokhlov, D. A. (1994). Vozniknovenie dvoiiinykh svyazyei kremnii-kremnii v plenkach a-Si:H, obluchennykh nyeonom i uglerodom pri otzhige. (The appearance of double silicon-silicon bonds in the a-Si:H films, exposed by neon and carbon during annealing). *Fizika i tekhnika poluprovodnikov. T.28, vyp.10. S.*, 1750-1754, in Russian.
- [30] Khokhlov, A. F., Pavlov, D. A., Mashin, A. I., & Mordvinova, Y. A. (1987). Izovalentnoe legirovanie amorphnogo kremniya uglerodom. (Isovalent doping of amorphous silicon by carbon). *Fizika i tekhnika poluprovodnikov, T.21, vyp.3*, 531-535, in Russian.
- [31] Lebedev, A. A., Mosina, G. N., Nikitina, I. P., Savkina, N. S., Sorokin, L. M., & Tregubova, A. C. (2001). Investigation of the structure of (p)3C - SiC-(n)6H-SiC. *Tech. Phys. Lett*, 27, 1052-1054.
- [32] Lebedev, A. A., Strel'chuk, A. M., Savkina, N. S., Bogdanova, E. V., Tregubova, A. S., Kuznetsov, A. N., & Sorokin, L. M. (2002). Investigation of the p<sup>3</sup>Cn-SiC/n<sup>+</sup>-6H-SiC heterostructures with modulated doping. *Tech. Phys. Lett*, 28(12), 1011-1014.
- [33] Lebedev, A. A., Nelson, D. K., Razbirin, B. S., Saidashev, I. I., Kuznetsov, A. N., & Cherenkov, A. E. (2005). Study of the properties of two-dimensional electron gas in p<sup>3</sup>Cn-SiC/n<sup>+</sup>-6H-SiC heterostructures at low temperatures. *Semiconductors*, 39(10), 194-996.
- [34] Lezhyeiko, L. V., & Lyubopytova, Ye. V. (1976). Svoistva p-n i n-n-geteroperekhodov Si- $\beta$ -SiC, poluchennykh ionnym vnedreniem. (Properties of p-n and n-n-heterojunctions Si- $\beta$ -SiC, obtained by ion implantation). *Fizika i tekhnika poluprovodnikov, T. 10, 6*, 1749, in Russian.
- [35] Liangdeng, Y., Intarasiri, S., Kamwanna, T., & Singkarat, S. (2008). Ion beam synthesis and modification of silicon carbide. In book "Ion beam applications in surface and bulk modification of insulators".- IAEA, Austria, Vienna, IAEA-TECDOC-1607, 63-92.
- [36] Liao, F., Girshick, S. L., Mook, W. M., Gerberich, W. W., & Zachariah, M. R. (2005). Superhard nanocrystalline silicon carbide films. *Appl. Phys. Lett*, 86, 171913-171915.
- [37] Lindner, J. K. N. (2003). High-dose carbon implantations into silicon: fundamental studies for new technological tricks. *Appl. Phys. A*, 77, 27-38.
- [38] Lyddane, R. H., Sachs, R. G., & Teller, E. (1941). On the polar vibration of alkali halides. *Phys. Rev*, 59, 673-676.
- [39] Morimoto, T., Ogura, Y., Kondo, M., & Ueda, T. (1995). Multilayer coating for carbon-composites. *Carbon*, 33(4), 351-357.



- [40] Mukhamedshina, D. M., & Beisenkhanov, N. B. (2012). Influence of Crystallization on the Properties of SnO<sub>2</sub> Thin Films. In book: "Advances in Crystallization Processes". Chapter 9. InTech. Dr. Yitzhak Mastai (Ed.), 219-258.
- [41] Nishino, S., Jacob, C., & Okui, Y. (2002). Lateral over-growth of 3C-SiC on patterned Si(111) substrates. *Journal of Crystal Growth*, 237-239, 1250-1253.
- [42] Oguri, K., & Sekigawa, T. (2004). Heat resistant material and hot structure member both space shuttle, space shuttle, and method for producing heat resistant material for space shuttle. *United State Patent* [US2004/0180242 A1], Sep.16.
- [43] Pajagopalan, T., Wang, X., Lanthouh, B., & Ramkumar, C. (2003). Low temperature deposition of nanocrystalline silicon carbide films by plasma enhanced chemical vapor deposition and their structural and optical characterization. *J. Appl. Phys*, 94(3), 5252-5260.
- [44] Pauling, L., & Pauling, P. (1975). Chemistry. *Freeman W.H. and company. San Francisco*.
- [45] Peierls, R. E. (1956). Quantum theory of solids. *Oxford: Clarendon Press*, 54-58.
- [46] Raabe, G., & Michl, J. (1985). Multiple Bonding to Silicon. *Chem. Rev.*, 85(5), 419-509.
- [47] Rothmund, W., & Fritzsche, C. R. (1974). Optical absorption and electrical conductivity of SiC films produced by ion implantation. *J. Electrochem. Soc.: Solid-state science and technology*, 121(4), 586-588.
- [48] Savkina, N. S., Lebedev, A. A., Davydov, D. V., Strelchuk, A. M., Tregubova, A. S., Raynaud, C., Chante, J. P., Locatelli, M. L., Planson, D., Nilan, J., Godignon, P., Campos, F. J., Nestres, N., Pascual, J., Brezeanu, G., & Batila, M. (2000). Low-doped 6H-SiC n-type epilayers grown by sublimation epitaxy. *Materials Science and Engineering*, B77, 50-54.
- [49] Semenov, A. V., Puzikov, V. M., Dobrotvorskaya, M. V., Fedorov, A. G., & Lopin, A. V. (2008). Nanocrystalline SiC films prepared by direct deposition of carbon and silicon ions. *Thin Solid Films*, 516(10), 2899-2903.
- [50] Semenov, A. V., Puzikov, V. M., Golubova, E. P., Baumer, V. N., & Dobrotvorskaya, M. V. (2009). Low-temperature production of silicon carbide films of different polytypes. *Semiconductors*, 43(5), 685-689.
- [51] Semenov, A. V., Lopin, A. V., Puzikov, V. M., Baumer, V. N., & Dmitruk, I. N. (2010). Fabrication of heterostructures based on layered nanocrystalline silicon carbide polytypes. *Semiconductors*, 44(6), 816-823.
- [52] Serre, C., Romano-Rodríguez, A., Pérez-Rodríguez, A., Morante, J. R., Fonseca, L., Acero, M. C., Kögler, R., & Skorupa, W. (1999). SiC on SiO<sub>2</sub> formed by ion implantation and bonding for micromechanics applications. *Sensors and Actuators A: Physical*, 74(1-3), 169-173.



- [53] Spillman, H., & Wilmott, P. R. (2000). Growth of SiN<sub>x</sub> and SiC<sub>x</sub> thin films by pulsed reactive crossed-beam laser ablation. *Applied Physics. A.- Materials Science & Processing*, 70(3), 323-327.
- [54] Spitzer, W. G., Kleinman, D., & Walsh, D. (1959). Infrared properties of hexagonal silicon carbide. *Phys. Rev.*, 113(1), 127-132.
- [55] Srikanth, K., Chu, M., Ashok, S., Nguyen, N., & Vedam, K. (1988). High-dose carbon ion implantation studies in silicon. *Thin Solid Films*, 323-329.
- [56] Sun, Y., & Miyasato, T. J. (1998). Characterization of cubic SiC films grown on thermally oxidized Si substrate. *J. Appl. Phys.*, 84(5), 2602-2611.
- [57] Tetelbaum, D. I., Mikhaylov, A. N., Belov, A. I., Vasiliev, V. K., Kovalev, A. I., Wainshtein, D. L., Golan, Y., & Oshero, A. (2009). Luminescence and structure of nanosized inclusions formed in SiO<sub>2</sub> layers under double implantation of silicon and carbon ions. *Journal of Surface Investigation. X-ray, Synchrotron and Neutron Techniques*, 3(5), 702-708.
- [58] Touriyanski, A. G., Aprelov, S. A., Gerasimenko, N. N., Pirshin, I. V., & Senkov, V. M. (2007). Otnositelnaya rentgenovskaya reflektometriya diskretnykh sloistykh struktur (Relative X-ray reflectometry of discrete layered structures). *Pis'ma v ZHTF (Technical Physics Letters)*, 33(5), 87-94.
- [59] Touriyanski, A. G., Gerasimenko, N. N., Aprelov, S. A., Pirshin, I. V., Poprygo, A. I., & Senkov, V. M. (2005). Investigation of ion-implanted layers by X-ray reflectometry. *Proc. SPIE. X-Ray and Neutron Capillary Optics II.*, 5943, 143-149.
- [60] Touryanski, A., Gerasimenko, N., Pirshin, I., & Senkov, V. (2009). Mnogofunktsionalnyi rentgenovskii reflektometr dlya issledovaniya nanostruktur (Multipurpose X-ray reflectometer for the study of nanostructures). *Nanoindustriya (Nanoindustry)*, 5, 40-45, in Russian.
- [61] Touryanski, A. G., Vinogradov, A. V., & Pirshin, I. V. (2000). X-ray reflectometer. *Patent no.6041098, US Cl. 378-70. Official Gazette March 21, 2000*, 2960.
- [62] Touryanski, A. G., Vinogradov, A. V., & Pirshin, I. V. (2000). Two-channel X-ray reflectometer. *Nucl. Instrum. and Meth. in Phys. Res.*, A 448, 184-187.
- [63] Yan, H., Wang, B., Song, X.M., Tan, L. W., Zhang, S. J., Chen, G. H., Wong, S. P., Kwok, R. W. M., & Leo, W. M. L. (2000). Study on SiC layers synthesized with carbon ion beam at low substrate temperature. *Diamond and related materials*, 9, 1795-1798.
- [64] West, R., Fink, M. J., & Michl, J. (1981). Tetramesityldisilene, a Stable Compound Containing a Silicon-Silicon Double Bond. *Science.*, 214, 1343-1344.
- [65] Williams, J. S., & Poate, J. M. (1984). *Ion Implantation and Beam Processing. Academic Press, Melbourne, 1984. Edited by Williams J.S., Poate J.M. 419 p., 30-31.*
- [66] Ziman, J. M. (1960). *Electrons and phonons. Oxford: Clarendon Press., 209.*

IntechOpen

IntechOpen